Renewable and Sustainable Energy Reviews 76 (2017) 1314–1331

Contents lists available at ScienceDirect

Renewable and Sustainable Energy Reviews

journal homepage: www.elsevier.com/locate/rser

Energy density and storage capacity cost comparison of conceptual solid and liquid sorption seasonal heat storage systems for low-temperature space heating

Luca Scapino[a,b,c,*], Herbert A. Zondag[b,d], Johan Van Bael[a,c], Jan Diriken[a,c], Camilo C.M. Rindt[b]

[a] VITO NV, Energy Technology unit, Thermal Systems Group, Boeretang 200 BE-2400 Mol, Belgium
[b] Eindhoven University of Technology, Department of Mechanical Engineering, P.O. Box 513 5600MB Eindhoven, The Netherlands
[c] EnergyVille, Thor Park 8300, 3600 Genk, Belgium
[d] ECN, Energy Research Center of the Netherlands, P.O. Box 1, 1755ZG Petten, The Netherlands

ARTICLE INFO

Keywords:
Sorption thermal energy storage
Solid sorption
Liquid sorption
Energy efficiency
Seasonal heat storage

ABSTRACT

Sorption heat storage can potentially store thermal energy for long time periods with a higher energy density compared to conventional storage technologies. A performance comparison in terms of energy density and storage capacity costs of different sorption system concepts used for seasonal heat storage is carried out. The reference scenario for the analysis consisted of satisfying the yearly heating demand of a passive house. Three salt hydrates ($MgCl_2$, Na_2S, and $SrBr_2$), one adsorbent (zeolite 13X) and one ideal composite based on $CaCl_2$, are used as active materials in solid sorption systems. One liquid sorption system based on NaOH is also considered in this analysis. The focus is on open solid sorption systems, which are compared with closed sorption systems and with the liquid sorption system. The main results show that, for the assumed reactor layouts, the closed solid sorption systems are generally more expensive compared to open systems. The use of the ideal composite represented a good compromise between energy density and storage capacity costs, assuming a sufficient hydrothermal stability. The ideal liquid system resulted more affordable in terms of reactor and active material costs but less compact compared to the systems based on the pure adsorbent and certain salt hydrates. Among the main conclusions, this analysis shows that the costs for the investigated ideal systems based on sorption reactions, even considering only the active material and the reactor material costs, are relatively high compared to the acceptable storage capacity costs defined for different users. However, acceptable storage capacity costs reflect the present market condition, and they can sensibly increase or decrease in a relatively short period due to for e.g. the variation of fossil fuels prices. Therefore, in the upcoming future, systems like the ones investigated in this work can become more competitive in the energy sector.

1. Introduction

Energy storage is one of the possible solutions for matching energy supply and demand in the future energy grid, in which intermittent and distributed energy production technologies will play an increasingly important role. In particular, energy storage is useful to increase the grid flexibility and safety, increase the amount of renewable energy sources, and improve the overall performance of energy systems [1].

Beside the previously mentioned benefits, and considering that the final energy use in domestic buildings is dominated by thermal energy (Fig. 1-1, bottom), thermal energy storage, or heat storage, can play a major role in reducing the primary energy consumption in buildings and in the future energy grid [2]. This is possible for example by decoupling the energy supply and demand sides, enabling the possibility to generate energy when it is more efficient and convenient, and store is till the time it is needed by the consumer.

Thermal energy storage can be divided into three main categories according to the storage mechanism: sensible, latent, and sorption heat storage. Sensible heat storage makes use of the temperature difference applied to a medium to store energy (e.g. water tank); latent heat storage exploits the phase change enthalpy of the medium, and sorption heat storage makes use of the reaction enthalpy involved in a typically reversible reaction.

The main advantages and drawbacks of the different technologies have been summarized in Table 1-1. Sensible storage is the most used and developed type of heat storage. For example, borehole heat storage

* Corresponding author at: Eindhoven University of Technology, Department of Mechanical Engineering, P.O. Box 513 5600MB Eindhoven, The Netherlands.
E-mail address: l.scapino@tue.nl (L. Scapino).

http://dx.doi.org/10.1016/j.rser.2017.03.101
Received 13 January 2017; Received in revised form 21 March 2017; Accepted 23 March 2017
Available online 06 April 2017

Nomenclature

Symbol description unit

$\dot{Q}$	Thermal power W
$\dot{m}$	Mass flow kg/s
A	Area m^2
b	Langmuir-Freundlich isotherm parameter 1/Pa
b_0	Langmuir-Freundlich isotherm parameter 1/Pa
C	Cost €
ESH	Yearly energy for space heating GJ
c_p	Specific heat capacity J/(kg·K)
D_p	Particle diameter mm
E	Volumetric energy density GJ/m^3
e	Specific energy density kJ/kg
G	Gibbs free energy kJ
H	Enthalpy kJ
h	Specific enthalpy kJ/kg
L	Length m
M	Molar mass g/mol
m	relative mass, Dimensionless
n	Langmuir-Freundlich isotherm parameter, Dimensionless
n_1	Langmuir-Freundlich isotherm parameter, Dimensionless
n_2	Langmuir-Freundlich isotherm parameter K
p	Pressure mbar
P	Power kW
q	molar concentration mol/kg
R	Ideal gas constant J/(mol·K)
R_{cryst}	Ratio of crystallization, Dimensionless
S	Entropy J/(kg·K)
T	Temperature °C
V	Volume m^3
W	Weight t
x	Relative mass concentration, Dimensionless
ε	Porosity, Dimensionless
η	Efficiency, Dimensionless
μ	Viscosity Pa·s
ρ	Density kg/m^3

Abbreviations

ANF	Annuity Factor
DHW	Domestic hot water
ENG	Expanded natural graphite
HCT	High concentration tank
HR	Heat recovery
LCT	Low concentration tank
REC	Reference energy cost
SCC	Storage capacity cost
ST	Sorbate tank

Subscripts and superscripts

cap	installed capacity
eq	Equilibrium
M	material
sol	solution
vap	Vapor

is able to store large amounts of energy over the year for space heating, but large volumes of storage material (water and soil) are required [3]. Latent heat storage has a higher energy density over a small temperature range. However, the materials cost is typically higher, and certain materials have corrosion and stability issues. Pielichowska et al. [4] give an overview of the present state of the art of phase change materials (PCMs) for thermal energy storage applications while Sharif et al. [5] focus in particular on PCMs for space heating and domestic hot water (DHW) systems. Sorption heat storage has the highest theoretical energy density among the three categories of heat storage, and the heat losses can be, in principle, negligible. This, in turn, can result in a more compact system, which makes this technology prone to be used to store large quantities of energy over a relatively long period. Main drawbacks are the materials instability issues at the current state of research, and the low maturity level of the technology, which implies that its commercialization is not foreseen in the near future.

Sorption thermal energy storage uses physical and chemical bonds between at least two components, sorbent and sorbate, to store thermal energy. During the desorption phase, heat is added in order to separate the sorbent and the sorbate with an endothermic reaction. During the sorption phase, the two components are combined together and heat is released with an exothermic reaction (Fig. 1-1, top).

Different sorption materials are investigated for the purpose of thermal energy storage for long-term and low-temperature applications. In particular, pure adsorbents and salt hydrates are mainly investigated by the scientific community for the abovementioned applications [8–12]. Salt hydrates have theoretically high energy densities but hydrothermal stability issues make the use of these materials in their pure form challenging, especially in open systems. On the other hand, adsorbents are more hydrothermally stable but they have typically lower energy densities and higher costs. The research on composite materials aims to reduce the material instabilities by keeping acceptable energy densities and costs. Composites generally consist of at least two materials, in which one is the active material that

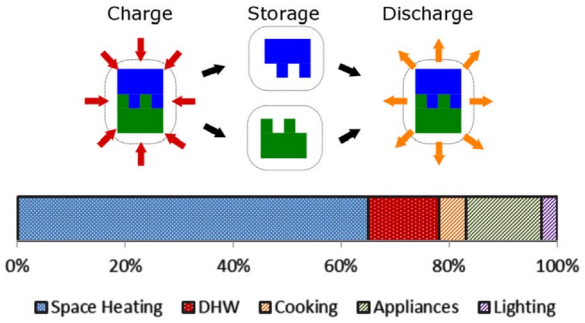

Fig. 1.1. Top: the sorption heat storage concept [6]. Bottom: End-use energy consumption of an household in EU (2012) [7]. Dotted bars: thermal energy; Striped bars: other forms of energy.

undergoes the sorption process and the other is mainly used for structural support. Beside the challenges at material-scale, at reactor- and system-scales, further issues such as heat and mass transfer through the reactor [13] and eventual components corrosion [14], have to be taken into account. Zondag [15] provides an introduction to sorption heat storage systems, with a particular emphasis on possible system configurations and overall system aspects. Abedin et al. [16] made a comparison among open and closed solid sorption systems based on energy and exergy analyses. The authors concluded that concerning charging, discharging and overall energy and exergy efficiencies, open systems were performing better than closed ones for the investigated cases. However, beside the thermodynamic factors, they suggested that other important factors such as economics have to be considered for the ultimate choice of a specific sorption heat storage system in a specific application. Hauer [17], discusses the possibilities and intrinsic limitations of sorption heat storage systems used for seasonal heat storage. Scapino et al. [18] gives an overview on the state of the art on sorption materials and existing sorption heat storage prototypes. Finally, Pinel et al. [19] and Xu et al. [20] provide an

Table 1.1
Thermal energy storage categories maturity levels [5] and main advantages and drawbacks (partially adapted from [6]). Maturity levels: 1= research and development; 2= demonstration and deployment; 3= commercialization.

Storage type	Maturity level	Advantages	Disadvantages
Sensible	3	Unhazardous and low cost material	Low energy density
		Relative simple system	Large volumes required
		Reliable	Self-discharge and heat losses
		Easy to control	High cost of site construction
			Geological requirements (ground storage)
Latent	2 – 3	Higher energy density than sensible heat storage	Lack of thermal stability
		Provide energy at almost constant temperature	Degradation
			Corrosion
			Material cost can be significant
Sorption	1	High energy density	Materials instability
		Compact system	Cyclability problems
		Negligible heat losses	Complex system
		Potentially non-toxic materials	Material cost can be significant

overview on seasonal heat storage technologies to store solar energy.

The objective of this work is to provide an estimation of ideal systems performance in terms of energy densities and storage capacity costs in a common reference scenario, assuming different active materials. The aim is to provide initial considerations about their techno-economic feasibility and competitiveness in the market. Special focus is on open systems based on solid/gas reactions with water as sorbate, which are then compared with closed systems and liquid absorption systems.

First, an ideal reference scenario is considered, with the aim to compare the systems at the same operating conditions. Then, for selected materials, the energy density is calculated according to the equilibrium curves (for salt hydrates) or adsorption isotherms/isoteres (for adsorbents). Afterwards, assumptions and estimations are made about the size of the systems and the auxiliary components needed, and cost estimations for the active materials and reactor materials are made. Finally, a comparison with closed systems and liquid sorption systems is made in terms of energy densities and active material costs by considering the acceptable storage capacity costs of three user classes: industry, building and the so-called energy enthusiast.

This analysis mainly focuses on the storage capacity costs in terms of active materials and reactor materials costs, without considering the auxiliary components, and systems dynamics. Additional important aspects to be considered in real systems are thermodynamic efficiencies during the systems operation, cost-sizing factors and relations among overall system costs and the main systems parameters, which are not included in the present work. For a proper investigation on some of the abovementioned aspects, especially techno-economic indicators, a higher maturity level of this technology is required.

2. Reference scenario, systems and materials

2.1. Reference scenario

A common application considered for the integration of a sorption heat storage system is a family passive-house, which has a space heating and domestic hot water demand, and solar thermal collectors on its roof able to provide the required desorption temperature. The aim of the sorption heat storage systems considered in this analysis is to store thermal energy during summer, and release it in winter to satisfy the space heating demand. This is the main concept of seasonal heat storage. Modern houses can make use of low temperature space heating systems such as floor heating, which can operate with supply temperatures below 40 °C [21]. This relatively low space heating temperature can be provided during the discharge phase of a sorption system operating within the boundary conditions listed in Table 2-1. On the contrary, if traditional heating systems would be present (e.g. heating temperatures of 70 °C) the use of sorption heat storage systems would become much more challenging. During the system discharge (sorption phase), evaporation heat from a low temperature source has to be provided in order to have a sufficient water vapor pressure at the system inlet. A borehole system, aquifer, surface water system, ambient air, or solar thermal collectors can cover this function. In order to test the systems at the same operating conditions, a reference scenario is defined. This implies that for all the systems analyzed, the same maximum temperature used to desorb the active materials and the same energy demand required from the consumer are assumed. Ferchaud et al. [22,23] and Zondag et al. [24] assumed a maximum temperature of 150 °C from the solar thermal collectors in similar analyses. The minimum system discharging temperature mainly depends on the applications. Low temperature space heating can make use of a temperature of approximately 40 °C. However, for DHW production, temperatures of 60 °C are normally required for prevention against legionella. In this scenario, only energy for space heating is considered, and a yearly demand (ESH) of 10 GJ is assumed [25]. The system has to store the entire amount of energy required (seasonal storage). Therefore, the thermal storage will perform only one sorption/desorption cycle per year. It is also assumed that the building is located in Amsterdam, the Netherlands, with 212 heating days per year (October - April), and that the low temperature heating system consumes a constant power during those days. The ambient temperature entering the system, i.e. after an eventual humidification system, is set at 10 °C. The main data of the reference scenario is presented in Table 2-1. Additional parameters assumed for this analysis, where not mentioned in the text, can be found in Appendix B.

Table 2-1
Reference scenario: passive house in Amsterdam (the Netherlands) with low temperature space heating and solar thermal collectors.

Reference Scenario Operating Conditions	
$T_{system\ charge}$ [°C]	150
$T_{space\ heating}$ [°C]	35/28
Energy space heating ESH [GJ/year]	10
Heating days	212
$T_{ambient}$ [°C]	10
$p_{H2O\ sat\ at\ Tambient}$ [mbar]	12.4

2.2. Systems investigated

This analysis focuses on three main types of sorption systems: open and closed solid sorption systems, and a liquid sorption system (Table 2–3).

In the open system configuration, during desorption, heat exchanger HX1 heats up the flow from a high temperature heat source, and valve V2 excludes the heat exchanger HX2. During the sorption mode, valve V1 excludes HX1 and valve V2 allows the flow through HX2 to transfer the heat to the appliances, and to the heat recovery unit.

In the closed system, during desorption, the heat exchanger HX3 is used to heat the material and separate sorbent and sorbate. The sorbate is then condensed in the sorbate tank by removing the condensation heat through HX4. During sorption, the sorbate is evaporated with

Table 2-2
Important general elements included and excluded in this analysis.

Included	Excluded
– Active materials volume and cost – Reactors material volume and cost	– Heat losses through the reactor walls – Auxiliary components – Thermodynamic efficiencies – Heat absorbed by reactor thermal mass

HX4 using a low temperature heat source, and the water vapor flows into the sorbent tank. Then, the reaction heat is removed from HX3 and sent to the appliances.

The liquid sorption system has a similar working principle to the closed solid sorption system. During the desorption mode, heat is provided in the absorber/desorber unit though HX5, and the sorbate is evaporated from the weak solution, which then becomes a strong solution, and is stored separately. During sorption, HX6 provides the required evaporation heat to transport the sorbate vapor into the absorber/desorber unit, in which the strong solution is flowing. This generates a weak solution and reaction heat, which is extracted through HX5.

Given the low maturity level of sorption heat storage systems, several assumptions are made throughout the analysis. For example, heat losses are not included in this analysis, since they are mostly dependent on the components design. Moreover, the heat absorbed by the reactor thermal mass is neglected. Table 2-2 summarizes the main general elements included and excluded in this analysis. Assumptions specific to a single system configuration, are presented elsewhere in the manuscript (i.e. Section 3 for open systems, Section 4 for closed systems, and Section 5 for liquid systems).

2.3. Active materials

The materials investigated in this assessment for solid sorption systems are three pure salt hydrates ($MgCl_2$, Na_2S and $SrBr_2$), one pure adsorbent (zeolite 13X), and one ideal composite. For the liquid sorption system, NaOH has been chosen (see Section 5.1). The boundary conditions of the reference scenario establish the achievable level of de/hydration for every material. Equilibrium curves in Appendix B (Fig. A-1) were estimated with NBS tables [26] to have a first estimation of the materials theoretical energy density. Additional assumptions at material level are shown in Table B-1. For every reaction step, the reaction enthalpy and entropy are calculated with the enthalpies and entropies of formation at standard conditions [26]. Then, equilibrium temperatures can be calculated according to equation (2.1):

$$\Delta G = \Delta H^0 - T\cdot\Delta S^0 + R\cdot T\cdot \ln Z \tag{2.1}$$

with

$$Z = \frac{\prod_i p_{product,i}}{\prod_i p_{reactant,i}} \tag{2.2}$$

Z is the ratio of the partial vapor pressures of products and reactants in the gas phase. The equilibrium curves can be calculated over a selected range of water vapor pressures, and in turn, a range of Z values. For every material, the equilibrium curves of relevant reaction steps are calculated (Fig. A-1) together with the energy densities referred to the material in the most hydrated form. As an example, the values for $MgCl_2$ are reported in Table 2–4. Data for the other materials are present in Appendix A.

From Table 2–4, a theoretical energy density of 2.49 GJ/m^3 can be seen for the material. However, in order to allow a proper mass transfer within the material, and to account for the material porosity, an effective bed porosity ε of 0.5 is assumed. The effective bed porosity halves the theoretical energy density that can be extracted from the material, supposed in a sorption reactor.

In order to estimate the energy density of zeolite 13X, adsorption isoteres (Fig. A-1) are calculated with the Langmuir-Freundlich isotherm.

$$q_{eq} = \frac{q_{max}\cdot b\cdot p^n}{1 + b\cdot p^n} \tag{2.3}$$

with

$$b = b_0\cdot e^{\left(\frac{\Delta E}{R\cdot T}\right)} \tag{2.4}$$

$$n = n_1 + \frac{n_2}{T} \tag{2.5}$$

q_{eq} represents the moles of water per kilogram of material adsorbed at equilibrium conditions, q_{max} the maximum amount of moles adsorbed per kilogram of material, p the water vapor pressure, R the gas constant, and T the temperature. The parameters used for the Langmuir-Freundlich isotherm are given in Table 2–5.

Assuming a desorption temperature of 150 °C, the maximum theoretical energy density achievable is 0.72 GJ/m^3. A bed porosity of 0.5 decreases the available energy density to 0.36 GJ/m^3. In order to estimate the maximum temperature lift achievable from the reaction steps, two different methods are applied. For closed systems, the equilibrium temperature is considered as the sorption temperature achievable within the reactor. If multiple reaction steps are present, the lowest equilibrium temperature is considered. For open systems, the lowest temperature increase between the previous approach and the "cp approximation" approach, showed in Eq. (2.6), is used. The latter assumes that all the water in the air reacts with the material, and that the energy released during the reaction is used to heat up the air mass flow. The temperature lift then becomes:

$$\Delta T = \frac{\rho_{vap}\cdot\Delta H}{M_{H_2O}\cdot\rho_{air}\cdot c_{p,air}} \tag{2.6}$$

with

$$\rho_{vap} = \frac{p_{H_2O}\cdot M_{H_2O}}{R\cdot T} \tag{2.7}$$

Here ρ_{vap} is the water vapor density, ΔH the average reaction enthalpy per mole of water, $c_{p,air}$ the air specific heat capacity, ρ_{air} the air density, p_{H2O} the water vapor pressure, M_{H_2O} the molar mass of water, R the gas constant, and T the temperature.

This assumption has been made based on two counterbalancing concepts. The first is that, in system based on multi-step reactions (e.g. $MgCl_2$), the reactor outlet temperature is typically higher than the lowest reaction equilibrium temperature because there are also other reaction steps contributing in the sorption process. The second is that the thermal losses in the components, that will decrease the reactor outlet temperature, have not been considered. Therefore, for a rough system approximation, the assumption used for the reactor outlet temperature represents a compromise between these two opposing effects.

For the closed system based on zeolite, it is assumed that the sorption temperature bed is kept at a temperature above the space heating required temperature, allowing 11 moles of water per kilogram of material to be released from the system discharge (Fig. A-1).

Finally, the performance of an ideal composite material is estimated, together with the related costs. For this analysis, the following assumptions are made:

- The composite is assumed to be made out of an inert hosting matrix and $CaCl_2$.
- The salt in its hexahydrate form occupies 50% of the material volume, and the other half of the volume is occupied by the hosting matrix.

Table 2–3
Basic schematic diagram of the investigated sorption systems configuration, main advantages and drawbacks. Partially adapted from [18].

	Open System	Closed System	Liquid system
Schematic Diagram	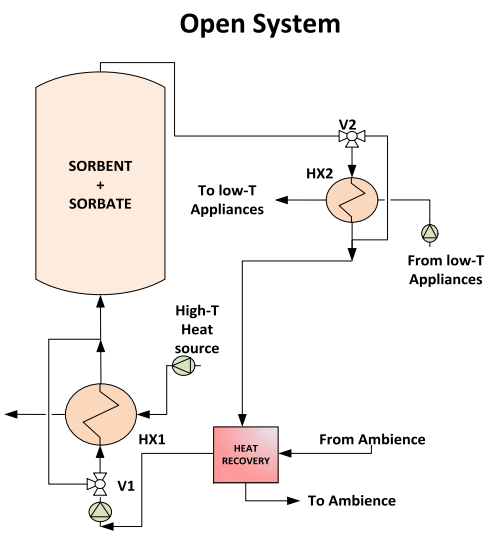	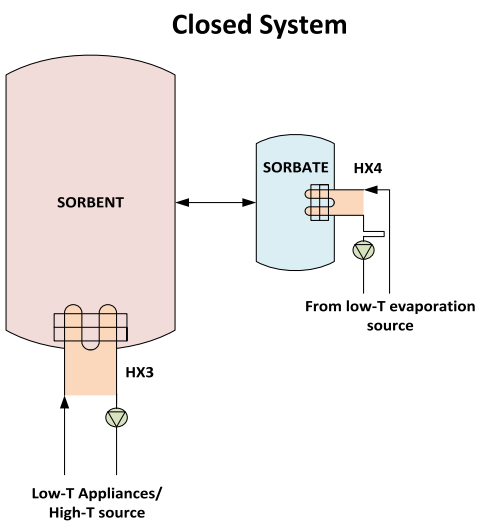	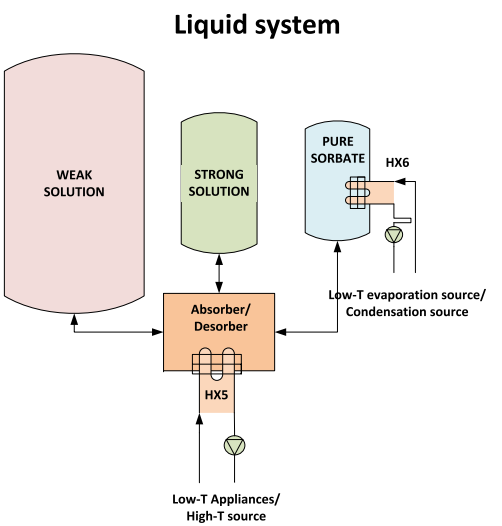
Advantages	• Atmospheric pressure • Simple system • Less components than for a closed system • Heat transfer increased by forced circulation	• Higher discharging temperature than for an pen system at similar vapor pressure • No mass exchange with environment • Can be used as an adsorption heat pump for cooling and heating	• No mass exchange with environment • Can be used as an adsorption heat pump for cooling and heating • Material easily stored and transported
Drawbacks	• Fan and humidifier often needed to drive the sorbate flow and provide partial humidification • Sorbate safety requirements • High sorbate flow leads to significant pressure drops • Mass transfer limiting step • Auxiliary energy required for fan operation	• Complex system • Condenser/evaporator required • Heat transfer limiting step • Sorbate needs to be stored • Periodical evacuation required • Sorbate evaporation energy to be fully provided • Large heat transfer area required in the reactor	• Condenser/evaporator required • Absorber/desorber required • Sorbate needs to be stored • Periodical evacuation to avoid non condensable gases • Sorbate evaporation energy to be fully provided

Table 2–4
$MgCl_2$ properties. Reaction enthalpy data from [26]. Investigated reaction steps: $MgCl_2 \cdot H_2O \leftrightarrow MgCl \cdot 2H_2O$, $MgCl_2 \cdot 2H_2O \leftrightarrow MgCl \cdot 4H_2O$, $MgCl_2 \cdot 4H_2O \leftrightarrow MgCl_2 \cdot 6H_2O$.

$MgCl_2$			
$\rho_{MgCl2 \cdot 6H2O}$ [kg/m^3]	1569		
$M_{MgCl2 \cdot 6H2O}$ [g/mol]	203.31		
Moles of water in solid phase	1↔2	2↔4	4↔6
mol(H_2O)	1	2	2
$\Delta H_{reaction}$ [kJ/mol(H_2O)]	71.27	67.82	58.2
mol(H_2O)/kg($MgCl_2 \cdot 6H_2O$)	4.92	9.84	9.84
T_{eq} [°C]	117.1	96.88	60.79
E [GJ/m^3($MgCl_2 \cdot 6H_2O$)]	0.55	1.05	0.90
E_{total} [GJ/m^3($MgCl_2 \cdot 6H_2O$)]	2.49		
$E_{bed,total}$ [GJ/m^3($MgCl_2 \cdot 6H_2O$)]	1.25		
$C_{active\ material}$ [€/t] [27]	154		

Table 2–5
Langmuir-Freundlich isotherm parameters for zeolite 13X [28].

n_1 [-]	−0.3615
n_2 [K]	274.23
q_{max} [mol/kg]	18
b_0 [1/Pa^n]	$308 \cdot 10^{-6}$
ΔE [J/mol]	18016

- The overall composite porosity is assumed 50%, as for the other materials investigated.
- The hosting matrix cost is assumed to be 600 €/t and its density 180 kg/m^3 [29].

Calcium chloride has been already investigated for sorption heat storage purposes [30] in its pure form [31], in composites [32–40], and in salts mixtures [41]. It is assumed that pure calcium chloride is unstable at the ambient temperature and water vapor pressure of the reference scenario, and deliquescence would occur [42]. It is assumed that the hosting matrix is able to retain efficiently the salt into its pores, therefore avoiding leakages of the active material. The density value of the hosting matrix is for expanded vermiculite, which has an intermediate density among the possible hosting matrices. In addition, the cost is assumed as an average value among various materials that can be used as hosting matrix. However, these values are highly dependent on the chosen material and its processing. The reactions relevant for sorption heat storage purposes at the reference scenario conditions are displayed in Table 2–6.

3. Performance estimation of open solid sorption systems

In an open system, the mass transfer of the sorbate through the sorbent is the main issue because pressure drops within the porous material can highly reduce the system efficiency. Therefore, the use of a reactor in which the air flows through the entire material amount at every system charge/discharge is not recommended. On the contrary, a modular or segmented configuration reduces the system pressure drops and the thermal mass of the material to be heated at every charge/discharge cycle. For a rough estimation of a module size, the following assumptions are made:

- Each segment can store the required space heating energy for one day.
- The energy released from the system is transferred to the space heating system with an air-water heat exchanger placed in a water tank that is able to deal with the daily fluctuations of the heat demand.
- Every module releases a constant energy flow through the day at a constant power. This energy is transferred to a low temperature heating system such as floor heating, which is not subjected to high peak energy demands, common for older high-temperature heating components.

The total amount of material can be divided into 212 batches, equal to the total amount of heating days per year (according to Section 2.1) that can be single modules or reactor segments. Considering the number of batches, and in order to minimize the amount of reactor material and maximize the reactor compactness, a segmented reactor has been chosen as layout for the open solid sorption system.

3.1. Reactor geometry and size estimation

In order to compare the active materials in a common reactor layout, it is assumed that a cubic reactor is divided into cuboids, and that every cuboid (segment) contains the energy required for one day of operation (Fig. 3-1). The result is a cubic reactor with 212 segments having the major length equal to one side of the cubic reactor.

This might not be the most suitable reactor layout for every sorption heat storage system, but in order to have a first rough comparison of the resulting pressure losses and the costs involved, this common arrangement is assumed. Further assumptions at reactor level are:

- Each cuboid is contained in a 1 mm stainless steel 316 shell. The choice of stainless steel in this analysis is assumed due to its corrosion resistance to the investigated salt hydrates [14]. The stainless steel density and cost are assumed to be 7740 kg/m^3 and 2.5 €/kg [43], respectively.
- The space heating heat exchanger is a cross flow heat exchanger, which can exploit the air energy from the reactor up to a temperature of 29 °C. An air-to-air heat recovery unit with an efficiency of 90% [44] is present between the inlet of the reactor and the outlet of the space heating heat exchanger.

The heat transfer medium in an open system is the gas flow (air) that contains the sorbate (water vapor). To estimate the required amount of active material needed, the daily amount of heated air has to be estimated depending on the maximum achievable temperature from the sorption heat storage system and the minimum air temperature achievable in the air-water heat exchanger.

$$\dot{m}_{air} = \frac{\dot{Q}_{HX,spaceheating}}{c_{p,air} \cdot (T_{air,HXin} - T_{air,HXout})} \tag{3.1}$$

Table 2–6
Ideal $CaCl_2$ composite properties. Reaction enthalpy data from [26]. Investigated reaction steps: $CaCl_2 \leftrightarrow CaCl_2 \cdot H_2O$, $CaCl_2 \cdot H_2O \leftrightarrow CaCl_2 \cdot 2H_2O$, $CaCl_2 \cdot 2H_2O \leftrightarrow CaCl_2 \cdot 4H_2O$.

$CaCl_2$ Composite			
$\rho_{CaCl2 \cdot 6H2O}$ [kg/m^3]	1710		
$M_{CaCl2 \cdot 6H2O}$ [g/mol]	219.08		
Moles of water in solid phase	0↔1	1↔2	2↔4
mol(H_2O)	1	1	2
$\Delta H_{reaction}$ [kJ/mol(H_2O)] [26]	73.93	51.63	61.14
mol(H_2O)/kg($CaCl_2 \cdot 6H_2O$)	4.56	4.56	9.13
T_{eq} [°C]	106.10	61.86	44.48
E [GJ/m^3($CaCl_2 \cdot 6H_2O$)]	0.58	0.40	0.95
ρ_{matrix} [kg/m^3]	180		
Volume of composite occupied by the salt [vol%]	50		
$\rho_{composite}$ [kg/m^3]	1136.5		
$E_{composite}$ [GJ/m^3($CaCl_2 \cdot 6H_2O$)]	0.97		
$E_{bed,total}$ [GJ/m^3($CaCl_2 \cdot 6H_2O$)]	0.49		
$C_{CaCl2 \cdot 6H2O}$ [27]	116		
C_{matrix} [€/t]	600		
$C_{active\ material}$ [€/t]	153		

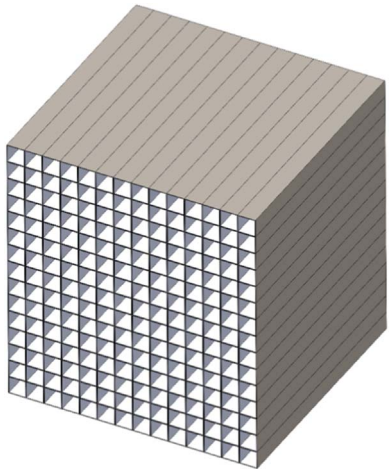

Fig. 3-1. Open system segmented reactor layout consisting of a set of cuboids equal to the amount of heating day in the reference scenario.

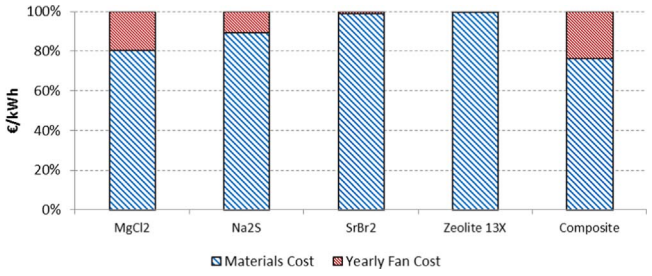

Fig. 3-2. Contribution of materials (sorption material + reactor material) cost and yearly fan consumption cost.

Then, it is assumed that a space heating system working at 35/28 °C receives the warm water from a water tank able to store the required daily amount of heat. According to the assumptions, a heat exchanger delivering a constant power of 546 W to the water tank during the system discharge is estimated. The constant power value is the result of the total yearly energy needed for space heating (10 GJ) divided over the heating days in the year. In Table 2-3 left, a schematic drawing of the assumed layout for an open solid sorption system is shown.

In order to recuperate the air released below 29 °C from the sorption heat storage, a heat recovery unit is present. Therefore, the ambient air is preheated and a higher outlet temperature from the reactor can be achieved. The preheated air temperature at the reactor inlet can be calculated as follows:

$$T_{air\ preheated,in} = T_{amb} + \eta_{HR}\cdot(T_{HX,out} - T_{amb}) \tag{3.2}$$

With η_{HR} the efficiency of the heat recovery unit, $T_{HX,out}$ the air temperature after the heat exchanger in the water tank, assumed to be 29 °C, and T_{amb} the ambient temperature at 10 °C. At those conditions, the preheated temperature is 27.1 °C. The inlet air humidity is assumed to be 12.4 mbar which is the saturated water vapor pressure at 10 °C. The sorption heat storage delivers the design constant power of 546 W above 29 °C to the air-water heat exchanger, then, it delivers low-temperature power used to preheat the ambient air. The reactor power can be computed by considering the temperature difference between its inlet and outlet air.

$$P_{reactor} = \dot{m}_{air}\cdot c_{p,air}\cdot(T_{reac,out} - T_{air\ preheated,in}) \tag{3.3}$$

In an open system, a source of energy consumption is the electrical power needed to drive the air mass flow, which can be estimated with the pressure drop through the reactor:

$$P_{fan} = \dot{V}_{air}\cdot\Delta p_{losses} \tag{3.4}$$

Table 3-1
Solid sorption open systems estimation of design parameters for the seven active materials investigated.

	$MgCl_2$	Na_2S	$SrBr_2$	Zeolite 13X	Composite
m_{air} [kg/s]	0.0201	0.0195	0.0253	0.0206	0,0351
$T_{air,max}$ [°C]	56.09	56.86	50.45	55.35	44.48
$P_{reactor}$ [W]	584	583	594	585	613
$E_{storage}$ [GJ/year]	10.70	10.68	10.89	10.72	11.23
$V_{reactor\ bed}$ [m^3]	8.56	7.66	11.11	29.78	23.03
$W_{reactor}$ [t]	6.72	6.05	13.25	15.49	10.88
V_{water}/V_M (ΔT= 50K)	5.52	6.19	4.28	1.59	2.07
$L_{segment}$ [m]	2.05	1.97	2.23	3.10	2.85
$A_{in/out,\ segment}$ [m^2]	0.0197	0.0183	0.0235	0.0453	0.0382
Δp [bar]	0.17	0.18	0.20	0.07	0.20
P_{fan}[W]	284	289	434	120	583
C_{fan} [€/year][a]	250	254	382	105	513
$C_{active\ material}$ [€/t]	154	348	2400	2500	153
$C_{materials}$ [€/kWh_{cap}]	0.79	1.16	11.90	14.57	1.18
$C_{materials+1\ year\ fan}$ [€/kWh·year]	0.88	1.25	12.04	14.61	1.36
$E_{reactor}$ [GJ/m^3]	1.17	1.31	0.90	0.34	0.43

[a] Considering an average electricity price of 0.173 €/kWh for a Dutch household in 2014 [47]

with $\dot{V}_{air}$ the air volume flow and Δp_{losses} the pressure losses within the reactor bed, estimated with the Ergun equation:

$$\frac{\Delta P}{L} = \frac{150\cdot\mu_{air}\cdot(1-\varepsilon)^2}{\varepsilon^3\cdot {D_p}^2}\cdot v_{air} + \frac{1.\ 75\cdot\rho_{air}\cdot(1-\varepsilon)}{\varepsilon^3\cdot D_p}\cdot {v_{air}}^2 \tag{3.5}$$

Where μ_{air} is the air viscosity, D_p is the particles diameter, assumed to be 1 mm, ρ_{air} the air density, and v_{air} the air velocity in the segment without active material.

The main results are visible in Table 3-1. The annual volume of materials required is in the range of 7.7–11.1 m^3 for salt hydrates, 29.8 m^3 for zeolite 13X, and 23 m^3 for the composite material. In order to store the same amount of energy with a temperature difference of ΔT=50 °C, a water storage of approximately 48 m^3 would be required.

The economic indicator considered in this work is the storage capacity cost (3.6), expressed in $€/kWh_{cap}$. In this analysis, this cost takes into account only the active material and the reactor material costs, and it is defined as:

$$SCC = \frac{reactor\ material\ cost + sorption\ material\ cost}{storage\ capacity} \tag{3.6}$$

In real systems, storage capacity costs should all the investment costs needed to realize the thermal energy storage system.

The salt hydrates appear to be the most interesting options in terms of energy densities.

- Sodium sulfide results to be the best option in terms of compactness, by having more than seven times the energy density than a conventional water storage. However, due to hazardousness of the material, it is not possible to use it in an open system configuration.
- Magnesium chloride results to be the best option in terms of active material costs by having it below 1 €/kWh_{cap}. However, from previous studies [22,45,46], it is known that the desorption temperature of the reference scenario (150 °C) will lead to material decomposition over the cycles. In order to reduce as much as possible the decomposition rate of $MgCl_2$, the desorption temperature could be decreased by exploiting only the first two reaction steps (6↔4 and 4↔2), resulting in a higher storage cost and a lower energy density. The relative fan energy costs for discharging the system during the winter season can account for 20% of the overall reactor and active material costs (Fig. 3-2). The relative fan costs appear to be more relevant with economic active materials (i.e. $MgCl_2$, Na_2S and the ideal composite), since they affect more the

overall system cost.

- Strontium bromide appears a promising alternative, resulting in a system approximately four times more compact than a water storage. However, due to the high material cost, the total cost of the sorption heat storage system is more than ten times higher compared to the one based on magnesium chloride.
- The zeolite storage requires a remarkably larger amount of material due to its lower energy density compared to pure salt hydrates. Considering also the high specific cost of the material, this leads to the most expensive options amongst the investigated systems.
- The composite material results in a more compact system compared to the system based on zeolite 13X, with an energy density of 0.43 GJ/m^3. From the economic point of view, the composite option is cheaper than zeolite 13X and $SrBr_2$, having a cost of 1.36 €/kWh_{cap}. This could be the most feasible option assuming a sufficient material stability given by the hosting matrix of the composite. Concerning the relative fan energy costs, they account approximately for 23%

3.2. Sensitivity analysis

In order to show the influence of the assumptions made, a sensitivity analysis on selected parameters is carried out. In the open system layout, the varied parameters are the heat recovery efficiency, the particle size diameter of the active material, and the reactor outlet temperature.

3.2.1. Heat recovery efficiency

The heat recovery unit is an essential part of the open system layout, since it significantly improves the overall system performance. The assumed heat recovery efficiency is 90%. However, real operational values can be far from the nominal one [44]. Thus, the heat recovery efficiency has been varied from 60% to 90% and the impact on the energy density and costs are estimated.

As it is possible to see in Fig. 3-3, the heat recovery efficiency has a remarkable effect on the energy density. A higher heat recovery efficiency results in higher achievable outlet reactor temperatures, and higher energy densities. Energy density variations of approximately 20% are present for pure salt hydrates, based on a heat recovery efficiency of 90%. Variations of 23% and 26% are found for the systems based on zeolite 13X and the ideal composite, respectively. Concerning the storage capacity costs, heat recovery efficiency affects more the cost of the systems based on the more expensive materials. A lower energy density implies larger quantities of material to be employed, therefore a higher materials cost is unavoidable. The importance of the heat recovery efficiency depends on the temperature difference between the two inlet flows (Eq. (3.3)), i.e. the larger the temperature difference between the two entering flows, the higher the importance of the HR efficiency. In this work, a temperature of 29 °C from the space heating heat exchanger and air at 10 °C from the ambient are assumed to enter the HR unit (Section 2.1), which implies a temperature difference of 19 °C.

3.2.2. Particle size diameter

The average particle size in the packed bed influences the pressure losses, as it can be seen from Eq. (3.5). This, in turn, has an influence on the system feasibility and its operational cost. In order to assess properly the impact of varying the particle size diameter on the system, the yearly operational costs due to the fan power are added to the storage capacity costs. Thus, if the system requires a too high amount of fan power to overcome the pressure losses, this will be taken into account in the cost assessment. The particle size has been varied between 0.1 mm and 5 mm, to have a particle size range going from fine powders to relatively large pellets. As it is possible to see from Fig. 3–4, by considering one year of system operation cost and the storage cost, particle size diameters of 0.1 mm considerably affect all the systems, leading to a cost increase from 15% (zeolite 13X) to 490% (composite) compared to the systems based on 1 mm particles. Larger particle sizes have a moderate effect on the cost.

3.2.3. Sorption temperature

A strong assumption is that the reactor outlet temperature for open systems corresponds to the lowest value between the lowest equilibrium reaction temperature and the temperature calculated with the "c_p approximation" (Eq. (2.6)).

Assuming that the thermal losses are minimized in a real system, it is interesting to estimate the systems performances if the reactor would be able to deliver the temperature based on the "cp approximation" approach. The systems in which the outlet temperature was already set as equal to the temperature found with the "cp approximation" approach ($MgCl_2$, Na_2S, and zeolite 13X), are also reported for comparison. From Fig. 3–5, it is possible to notice the substantial temperature increase for all the materials.

The increase of temperature is 5% ($SrBr_2$) and 23% (composite), compared to the original outlet temperature. Consequently, the air flows through the reactor have a decrease of −11% ($SrBr_2$) and −40% (composite) compared to the original air flows. This is because the power that has to be provided from the reactor to the space heating system remains the same. In Fig. 3-6, the storage costs by varying the outlet temperature are displayed and divided between storage capacity costs and yearly fan operational costs. Overall, a general cost decrease is present due to lower operational costs caused by the reduction of the air flow, and the higher energy densities affecting the storage capacity cost. Finally, the systems energy density (Fig. 3-7) increases of 0.9% ($SrBr_2$) and 4.6% (composite) because of lower amount of material required since a lower amount of sorbate (water vapor) flows through the reactor and depletes the sorption material.

4. Performance comparison with closed solid sorption systems

In the following section, the performance of different closed solid sorption systems based on the previously introduced active materials are estimated (Section 4.1). Then, a comparison between open and closed solid sorption systems is made in terms of reactor energy density and storage capacity cost (Section 4.2). Finally, a sensitivity analysis on the ideal composite material parameters (Section 4.3) is carried out with the aim to understand the influence of these parameters on the energy density and storage capacity cost of the reactor.

4.1. Performance estimation of closed solid sorption systems

A closed system requires additional components compared to an open system. During the system discharge, an evaporator is needed to evaporate the sorption water that subsequently reacts with the active material. During the system charge, a condenser is required to condense the sorbate vapor removed from the active material. Differently from an absorption heat pump, the two phenomena do not happen simultaneously; therefore, if properly designed, the condenser and evaporator can be the same component. In this analysis, the

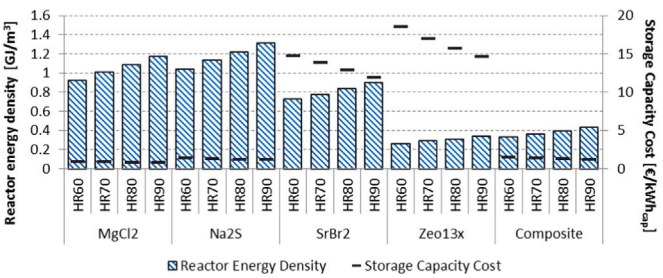

Fig. 3-3. Energy density and storage cost variation by varying the heat recovery efficiency (HR) from 60% to 90%.

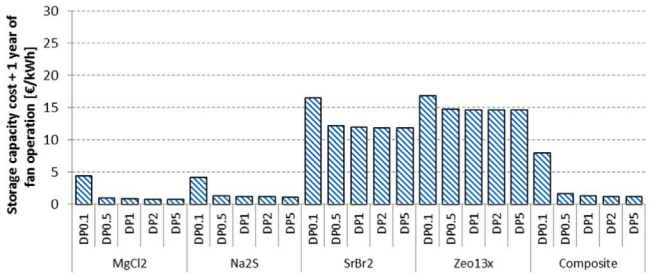

Fig. 3–4. Storage capacity cost and one year of fan operational cost by varying the particle size diameter from 0.1 to 5 mm.

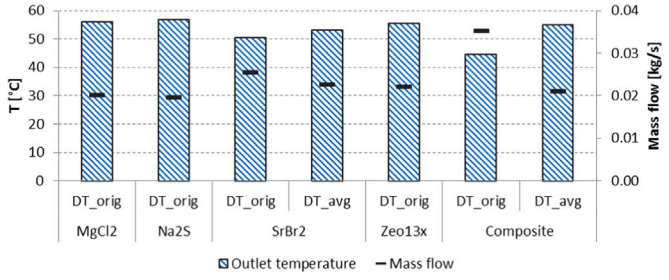

Fig. 3–5. Reactor outlet temperatures and mass flows assuming the lowest equilibrium temperature (DT_orig) or the "cp approximation" approach (DT_avg) for $SrBr_2$ and the ideal composite material. Data for $MgCl_2$, Na_2S and zeolite 13X already based on the "cp approximation" approach are added for comparison.

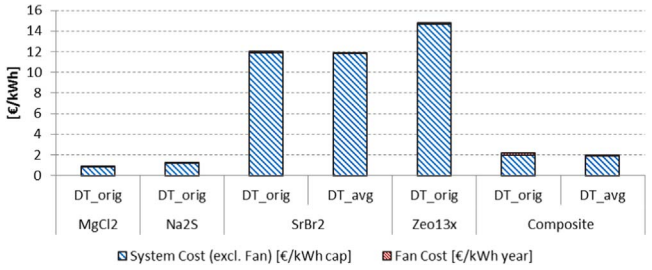

Fig. 3–6. Storage costs and operational costs varying the reactor outlet temperature assuming the lowest equilibrium temperature (DT_orig) or the "cp approximation" approach (DT_avg) for $SrBr_2$ and the ideal composite material. Data for $MgCl_2$, Na_2S and zeolite 13X already based on the "cp approximation" approach are added for comparison.

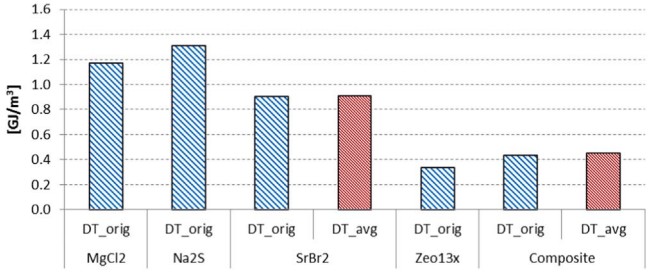

Fig. 3–7. Energy density varying the reactor outlet temperature assuming the lowest equilibrium temperature (DT_orig) in blue and an averaged outlet temperature (DT_avg) in red for $SrBr_2$ and the ideal composite material. Data for $MgCl_2$, Na_2S and zeolite 13X already based on the "cp approximation" approach are added for comparison.

heat removed during condensation will be lost and it will not be considered as additional value. Finally, closed systems can require frequent evacuation due to the formation of incondensable gases. This requires additional energy to run the evacuation pumps. This aspect is not considered in this analysis.

The closed system requires a storage volume for the sorbate, which is not released into the environment as for an open system. As a rough system size estimation, the following assumptions are made:

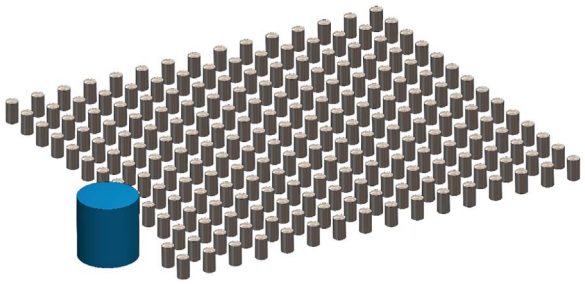

Fig. 4-1. Closed system layout assumed for every sorption material. Every active material tank contains the required amount of energy for one day of operation and the water tank contains the sorbate necessary for one year of operation.

- The volume of the evaporator/condenser heat exchanger is not significant compared to the active material volume and the required sorbate volume. Therefore, it will not be taken into account.
- The sorbent and the sorbate are contained into cylindrical shells with a diameter of 0.3 m and 1.5 m, respectively.
- The active material is divided into modules in which the daily energy demand is stored (Fig. 4-1).
- At the sides of each cylindrical there is a cap with a height of 0.05 m.
- The material for the reactor is stainless steel 316, and the container thicknesses are 3 mm and 2 mm for the modules and the sorbate container, respectively.
- The heat transfer area between the water for the space heating system and the active material in every module is not taken into account.
- The energy is efficiently removed from the reactor bed by the heat exchanger. Therefore, all the energy released is transferred to the space heating system.

The heat transfer area between the water for the space heating system and the active material in every module is not considered because it is strongly dependent on the heat exchanger shape, the heat transfer coefficient between the sorption bed and the fluid inside the heat exchanger, and the temperature of the sorption bed. In particular, the latter is dependent on the amount of water vapor flowing through the bed, which in turn depends on the pressure difference between the evaporator and the sorption bed, which is not constant. Therefore, a numerical model valid for only one single material and reactor shape would be required, and it is out of the scope for a rough size estimation of the system. In reality, the volume of the heat exchanger in each module has also to be considered. With the abovementioned assumptions, the results of the system estimation are visible in Table 4-1. The sorbate volume to be stored depends on the moles of water involved in the sorption reactions for every material. The overall sorbent and sorbate volumes range from 9.9 m^3 (Na_2S) to 13.3 m^3 ($SrBr_2$) for the pure salt hydrates, 28.5 m^3 for zeolite 13X, and 23.4 m^3 for the composite. Pure salt hydrates ($MgCl_2$ and Na_2S) represent the least expensive solutions, followed by the ideal composite. The pure adsorbent is again the most expensive option among the investigated ones. The storage capacity costs, considering the active material and the reactor material costs, have a range of 2.97 €/kWh_{cap} ($MgCl_2$) to 13.67 €/kWh_{cap} ($SrBr_2$) for salt hydrates, 6.69 €/kWh_{cap} for the ideal composite and 19.48 €/kWh_{cap} for the zeolite 13X system. It has to be recalled that in this analysis the heat exchanger volume inside the active material tanks is not taken into account, and it would contribute to increase the overall system cost and volume occupied, thereby decreasing the energy density.

4.2. Comparison between open and closed solid sorption systems

From a first estimation of the sizes of both open and closed systems based on three salts hydrates, zeolite 13X, and an ideal composite, it is possible to draw preliminary conclusions on the systems performances

Table 4-1
Design parameters of a closed sorption system varying the active material.

	$MgCl_2$	Na_2S	$SrBr_2$	Zeolite 13X	Composite
$V_{reactor\ bed}$ [m^3]	8.00	7.17	10.20	25.64	20.51
$V_{sorbate}$ [m^3]	2.78	2.73	3.09	2.86	2.91
$V_{sorbate+reactor\ bed}$	10.78	9.90	13.29	28.5	23.42
V_{water}/V_M (ΔT= 50K)	4.43	4.83	3.59	1.68	2.04
Active Material Tanks Estimation					
$W_{tank,\ active\ material}$ [kg]	42.5	37.8	73.0	101.3	77.1
$L_{tank,\ active\ material}$ [m]	0.53	0.48	0.68	1.71	1.37
$W_{tanks,\ active\ material}$ [t]	9.0	8.0	15.5	21.5	16.3
Sorbate Water Tank Estimation					
$L_{sorbate\ storage}$[m]	1.58	1.55	1.75	1.62	1.64
$W_{sorbate\ storage}$ [t]	2.96	2.90	3.29	3.04	3.09
Energy density and storage capacity costs estimation					
$C_{materials}$[€/kWh_{cap}]	2.97	2.99	13.67	19.48	6.69
$E_{reactor}$ [GJ/m^3]	0.90	0.98	0.73	0.34	0.41

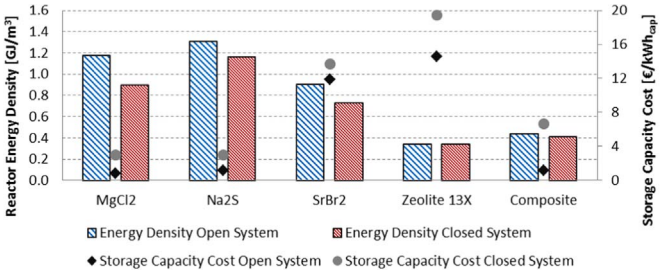

Fig. 4-2. Open and closed systems comparison in terms of systems energy density and storage capacity cost.

and storage capacity costs defined as the ratio of the system costs and the installed storage capacities. The system costs considered are the active materials and the main reactor material costs. From Fig. 4-2, it is possible to notice that the energy densities of open systems are higher. This is because the closed systems require the sorbate to be stored, therefore increasing the overall system volume. Additionally, for pure salt hydrates, the assumed open system layout is more compact whereas the closed system is divided into a number of tanks equal to the yearly heating days. The large amount of tanks implies also a large use of reactor material; thereby increasing the system capacity costs. In particular, this is remarkable in the zeolite system, which requires a relatively large amount of reactor material, because of the relatively low material energy density, resulting in the highest storage capacity cost.

For zeolite 13X, the energy density of the closed system layout is slightly higher because the volume required to store the active material and the sorbate is lower compared to the volume to store the active material in the open system layout. This is because in the open system, part of the energy stored is lost to the environment in the heat recovery unit (Table 2-3); while for the closed system, it is assumed that the energy is entirely transferred to the space heating system. Thus, in an open system, more material is needed compared to a closed system, and if the material energy density is low enough, it can be that the required additional volume of the material in the open system is larger than the volume required in the closed system to store both the active material and the sorbate (water).

Systems based on the composite material have energy densities above the systems based on pure adsorbents (0.43 – 0.41 GJ/m^3), with a slightly higher value for open systems. Moreover, their storage capacity costs are remarkably lower being approximately 6 – 12 times lower for closed and open systems, respectively.

Concerning the storage capacity costs, open systems resulted in lower costs compared to closed systems. This is because the reactor layout assumed for the closed systems requires more material compared to an open system. In Fig. 4-3, the reactor material cost percentage related to the overall materials costs for open and closed sorption systems is shown, and it is remarkably higher for closed systems, in particular for the most compact and inexpensive systems.

This means that, for the systems in which the reactor material cost heavily affects the overall system cost, the choice of a suitable and inexpensive material is essential.

4.3. Sensitivity analysis on composite material parameters

Two of the main parameters of the composite material that affect the investigated system performance are the amount of active material present in the composite and the hosting matrix price. By varying the amount of active material, the overall energy density is directly affected (Fig. 4-4). The amount of active material in the composite is varied between 20 vol% and 80 vol% for both open and closed systems layouts. Assuming a hosting matrix density of 180 kg/m^3, volume fractions of 20 – 80 vol% would correspond to weight fractions of approximately 70–97 wt%, respectively. For comparison, values of 90 wt% of $CaCl_2$ are achieved for composites with ENG matrices [33,48]. A substantial and proportional increase in the energy density is present by increasing the amount of active material in the ideal composite. For open systems, the energy density variation is in the range from −60% (20 vol%) to +63% (80 vol%) compared to the 50 vol % case. For closed system, the range is within −56% – +49% for the same volume percentage of active material in the composite. It can be noticed that, by increasing the amount of active material, the energy density increase is sharper in open systems. This is due to the chosen layouts and assumptions in open and closed systems estimation, which in turn result in different amounts of reactor material required for open and closed system layouts.

Concerning the storage capacity costs, closed systems have larger amounts of reactor material (Fig. 4-3) and their costs decrease more

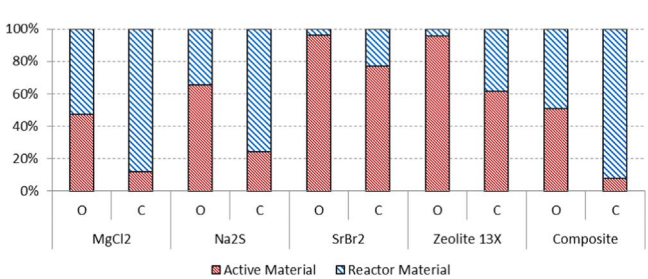

Fig. 4-3. Reactor and active materials costs ratio for open (O) and closed (C) solid sorption systems.

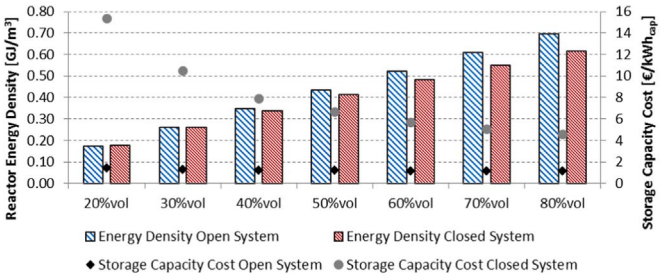

Fig. 4-4. Open and closed systems comparison for different amounts of active material in the composite material.

rapidly by increasing the amount of active material in the composite. Its nonlinear tendency is due to the mutual effects between the decrease of composite material required by increasing the amount of active material in the composite, and the consequent lower amount of reactor material required. Closed systems have a cost range within +131% (20 vol%) and − 32% (80 vol%) and open systems between +20% and − 2.5% for the same active material percentages, referred to the costs at 50 vol% of active material under the present assumptions.

Concerning the hosting matrix price, its value has been varied between ± 75% of the initial value (600 €/t) to investigate its influence on the storage capacity costs of the systems. The results can be seen in Fig. 4–5. As expected, a linear behavior in the storage capacity costs is present for both open and closed systems. For open systems, a range of ± 13.5% of the matrix price, compared to the original matrix price, is estimated. For closed systems this range is within ± 2.1%. A smaller influence of the matrix price in closed systems is due to the fact that they are more influenced by the reactor material costs (Fig. 4-3).

5. Performance comparison with liquid sorption systems

In order to have a general overview of the liquid sorption systems performance and their suitability for the assumed reference scenario, four absorption couples from the literature are analyzed. Then, an ideal liquid sorption system is defined in this work (5.2). Finally, the previously estimated open and closed solid sorption systems are compared in terms of energy density and storage capacity cost with the liquid sorption system estimated in this Section (5.3).

5.1. Liquid sorption systems from the literature

In order to estimate an ideal liquid sorption system to compare with the previously estimated solid sorption systems, different absorption couples from Liu et al. [49,50] are considered. General literature references and state of the art reviews on liquid absorption technologies can be found in [51–53] . The data from the study of Liu et al. [50] have been used to define the sorption cycle of a typical system based on the most suitable absorption couple for the reference scenario in 2.1. Possible absorption temperatures in the range of 20 – 45 °C have been investigated by the authors assuming an evaporator temperature of 10 °C and a sorbate storage temperature of 10 °C. However, not all the absorption couples were able to release heat above 35 °C, the space heating system requirement in the reference scenario.

In Table 5-1, the energy density of different absorbents, at the stated absorber temperature are reported in case of no crystallization allowed in the storage tank, or a ratio of crystallization equal to 4. The energy density is given considering one cubic meter of pure absorbent material. The ratio of crystallization (R_{cryst}) is defined as the mass ratio of crystal in the storage tank present at the end of the storage period and the mass ratio of solution at the same state. A ratio of crystallization equal to 4 implies that there is 20% of liquid solution in the storage tank at the beginning of the absorption cycle, which has to be high enough to allow the solution recirculation in the absorber at the beginning of the discharge process. As it can be seen in Table 5-1, the active material volume required by a single stage liquid absorption system operating in the reference scenario varies from 5.8 to 18.9 m^3 or from 2.31 to 9.39 m^3 with R_{cryst}=0 or R_{cryst}=4, respectively. The maximum absorption temperature at which the storage process has a significant energy density is 35 °C for three of the four absorption couples investigated (LiBr-H_2O, LiCl-H_2O, KOH-H_2O), which is realistically not enough to achieve 35 °C on the space heating side, considering the system thermal losses and the heat exchanger effectiveness. By increasing the absorber temperature in those absorption couples a too small absorbent concentration difference, e.g. lower than 5% for the LiBr-H_2O couple, would result in the system. Only the system based on NaOH-H_2O has been investigated at higher absorption temperatures, and it resulted in a relatively low energy density. The resulting active material cost of the only feasible single stage liquid sorption system based on NaOH are 5.76 and 2.88 €/kWh_{cap} with or without partial recrystallization respectively (Table 5-1). Finally, it is remarkable that the required desorption temperature from the liquid sorption systems is lower compared to solid sorption systems. In particular, according to the authors, the system based on NaOH-H_2O that they considered, required 50 °C (p_{H2O}=4.2 kPa) to be charged, assuming R_{cryst} =0.

5.2. Ideal liquid sorption system estimation

From the data of the previous paragraph, it appears that a NaOH-H_2O system can deliver the energy above the minimum temperature required in the reference scenario. Therefore, a first rough estimation of this system operating in the reference scenario is carried out in Appendix C with the aim to compare it with the solid sorption systems performance. A minimum useful temperature of 35 °C is set even though, at realistic operating conditions, a higher temperature has to be provided in order to have 35 °C at the space heating system side. The assumptions of this analysis are displayed in Table 5-2, and the main results are displayed in Table 5-3. A similar procedure to the one employed by Liu et al. [50] is adopted.

It is interesting to notice the remarkable energy density reduction if the required tanks volume and the reactor material is taken into account. In Fig. 5-1, the energy density based on the pure absorption material of the absorption couples taken from the literature (5.1) and the liquid sorption system based on NaOH estimated in this section are shown. It is possible to see that for the system based on NaOH taken from the literature, a lower pure absorbent energy density E_{NaOH} (0.53 GJ/m^3) is present due to the considered minimum heat release temperature of 45 °C, while for the system estimated in this section (2.18 GJ/m^3) the minimum heat release temperature was set at 35 °C, according to the reference scenario in Table 5-2.

For the ideal NaOH system estimated in this section, the energy density based on the required tanks volume and the costs including also the reactor material is also displayed (red marker) and calculated in Appendix C. It is possible to see the strong decrease (−91%) in the energy density due to the required volume of water involved in the process, which determines the strong solution, weak solution and pure

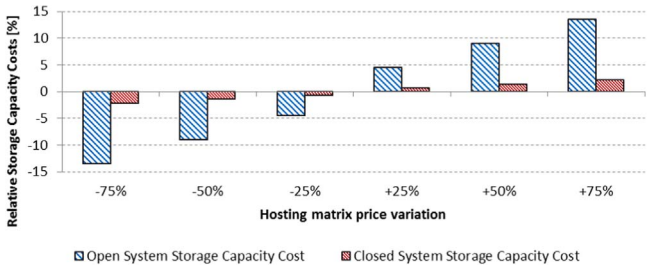

Fig. 4–5. Open and closed systems comparison varying the composite hosting matrix price. Closed systems are less sensible to hosting matrix price variation due to the higher influence of the reactor material cost.

Table 5-1
Different absorption couples, with or without partial crystallization in the storage tank [50].

	LiBr-H_2O	NaOH-H_2O	LiCl-H_2O	KOH-H_2O
$T_{absorption}$ [°C]	35	45	35	35
$T_{desorption,Rcryst=0}$[a] [°C]	72	50	66	63
$T_{desorption,Rcryst=4}$[a] [°C]	78	57	93	84
Storage capacity R_{cryst}= 0 [kJ/$kg_{absorbent}$]	500	250	750	250
Storage capacity R_{cryst} = 4 [kJ/$kg_{absorbent}$]	1250	500	1650	1000
$\rho_{absorbent}$ [kg/m^3]	3460	2130	2070	2120
$E_{absorbent,Rcryst=0}$ [$GJ/m^3_{active\ material}$]	1.73	0.53	1.55	0.53
$E_{absorbent,Rcryst=4}$ [$GJ/m^3_{active\ material}$]	4.33	1.07	3.42	2.12
$V_{absorbent,Rcryst=0}$ [m^3]	5.78	18.78	6.44	18.87
$V_{absorbent,Rcryst=4}$ [m^3]	2.31	9.39	2.93	4.72
$C_{absorbent,specific}$ [54] [€/t]	5500	400	2700	1200
$C_{absorbent,Rcryst=0}$ [k€]	110	16	36	48
$C_{absorbent,Rcryst=4}$ [k€]	44	8	16	12
$C_{storage,Rcryst=0}$ [€/kWh_{cap}]	39.6	5.76	12.96	17.28
$C_{storage,Rcryst=4}$ [€/kWh_{cap}]	15.84	2.88	5.89	4.32

[a] Assuming a condenser vapor pressure of 4.2 kPa.

Table 5-2
Assumptions for the liquid sorption system estimation.

Evaporator temperature T_{eva} [°C]	10
Minimum storage temperature $T_{storage}$ [°C]	10
Useful heat temperature [°C]	> 35

Table 5-3
Main parameters of the liquid sorption system based on NaOH-H_2O.

E_{NaOH} [GJ/m^3]	2.18
$E_{sol,system}$ [GJ/m^3]	0.20
$C_{SSC,\ NaOH+tanks}$ [€/kWh_{cap}]	1.44

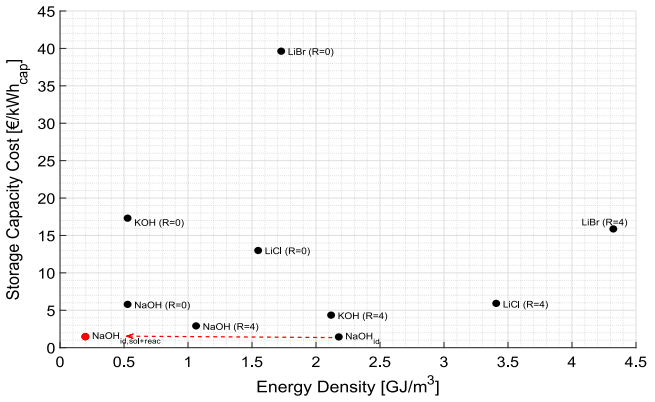

Fig. 5-1. Energy density and costs of liquid sorption materials from the literature and the estimated NaOH liquid sorption system based on the pure absorbent energy density (black markers). The red marker indicates the solution + reactor material volume energy density of the ideal liquid sorption system based on NaOH. (For interpretation of the references to color in this figure legend, the reader is referred to the web version of this article.)

sorbate tanks volume. A significant decrease in energy density is expected also for the absorption couples from the literature, if the required tanks volume is taken into account. Equations from (C.2) to (C.7) in Appendix C illustrate how to derive the ideal system energy density considering the tanks volume from the pure absorbent energy density.

For the comparison with the ideal solid sorption systems estimated in this analysis (Sections 3 and 4), only the ideal NaOH-H_2O system, considering also the tanks volume and cost, is considered.

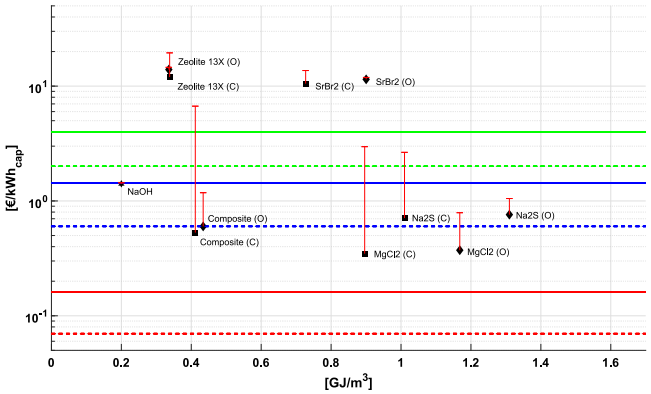

Fig. 5-2. Materials energy density vs active material costs (markers) and active materials + reactor material costs (red vertical lines). Marker types: Rhomboids=Open systems (O), Squares= closed systems (C), Hexagram=ideal liquid sorption system. Minimum (dashed line) and maximum (solid line) acceptable storage capacity costs of a thermal storage operating one cycle per year [56] for industry (red), building (blue) and enthusiast (green) users. (For interpretation of the references to color in this figure legend, the reader is referred to the web version of this article.)

5.3. Comparison between solid and liquid sorption systems

In Fig. 5-2, a comparison amongst the solid sorption systems and the liquid sorption system is shown. The cost of the active materials is represented by the markers and the cost increase due to the reactor material is represented by the vertical red lines. Auxiliary system components and the system operation costs would increase further the system costs and decrease the overall energy density. For solid sorption open systems, only the sorbent volume is considered since the sorbate is not stored. For the liquid sorption system estimated in this analysis, the energy density is referred to the volume occupied by the solution during the process (V_{HCT} V_{LCT} V_{ST}). Open and closed systems have already been discussed in 4.2, and they have comparable energy densities amongst the pure salt hydrates: 0.90–1.31 and 0.73 - 1.16 GJ/m^3 for open and closed systems, respectively. Lower energy densities are instead present for the open systems (0.33 – 0.43 GJ/m^3) and the closed systems (0.35 – 0.43 GJ/m^3) based on zeolite 13X and on the ideal composite, respectively. The liquid sorption system based on NaOH has an energy density of 0.20 GJ/m^3. Rathgeber et al. [55,56], within the framework of IEA SHC Task 42/ ECES Annex 29, made an economic evaluation of thermal energy storages, and set the economic boundaries for different user categories: industries, buildings and enthusiasts. Industries can accept payback periods of 5 years and interest rates on the capital costs of 10%; buildings can accept payback periods of 15 – 20 years and interest rates of 5% and enthusiasts can accept interest rates of 1% and payback periods of 25 years. With the interest rates on the capital costs and the acceptable payback periods of the user classes, the acceptable annuity factors can be estimated. Another indicator considered in the economic evaluation are the reference energy costs (REC) which represent the cost of energy supplied from the market. The assumption of the authors was that the costs of the energy supplied by a thermal energy storage should not exceed the costs of the same energy supplied from the market. It is noteworthy to mention that they depend on many external factors such as the economic and political conditions of each country; therefore are variable within relatively short time periods. The authors considered a range of REC and annuity factors (ANF) for every class user, and estimated the acceptable storage capacity costs (SCC_{acc}) of different existing thermal energy storages with Eq. (5.1). The results are visible in Table 5-4.

$$SCC_{acc} = \frac{REC \cdot N_{cycle}}{ANF} \tag{5.1}$$

Table 5-4
Acceptable storage capacity costs for one system cycle per year [56].

User Class	REC [€/kWh]	ANF [1/y]	SCC_{acc} [€/kWh_{cap}]
Industry	0.02 – 0.04	0.25 – 0.30	0.07–0.16
Building	0.06 – 0.10	0.07 – 0.10	0.60–1.43
Enthusiast	0.12 – 0.16	0.04 – 0.06	2–4

The acceptable storage capacity costs are defined in function of the substituted reference energy costs, the annuity factors, and the number of yearly cycles that the thermal storage undergoes. Since in this analysis only seasonal thermal energy storages are considered, only one annual cycle is performed. In Fig. 5-2, the range of acceptable storage capacity costs by the three different users defined by the authors are displayed assuming one charging/discharging cycle of the systems every year.

Based on the results of Fig. 5-2, it is possible to notice that the active material costs of the investigated systems are not competitive for an industrial user. For building users, some of the systems based on pure salt hydrates ($MgCl_2$ and Na_2S) are within the acceptable storage capacity costs by considering only their active material cost. However, as already mentioned, their hydrothermal stability issues (e.g. $MgCl_2$) make these systems hardly feasible. Moreover, open systems based on Na_2S, face environmental issues due to the toxicity of the salt hydrate and its byproducts such as hydrogen sulfide. Therefore, only closed systems based on Na_2S are advisable. However, the production of non-condensable gases during the system operation decreases the system efficiency; therefore, they have to be periodically removed to keep the system pressure at optimal levels.

The systems based on the ideal composite material, assuming a sufficient material stability, would represent a promising option since they have relatively low storage capacity costs (0.60 – 0.53 €/kWh_{cap} for the closed and open system, respectively) affordable for the buildings category. However, they would result also in approximately two and a half times larger systems compared to the open system based on pure $MgCl_2$.

The liquid sorption system estimated in Section 5.2 , having an energy density of 0.20 GJ/m^3 released at a temperature above 35 °C has active material costs within the acceptable storage capacity costs of the building users (1.44 €/kWh_{cap}).

Finally, the solid systems based on strontium bromide and zeolite 13X resulted above the storage capacity costs affordable from all the user categories (10.0–14.6 €/kWh_{cap}). In case of applications requiring more charge/discharge cycles per year, their costs can decrease and they might become affordable for the investigated user categories.

Considering also the reactor material costs estimated in this analysis, by looking at the vertical red lines in Fig. 5-2, it is possible to notice that solid sorption systems, especially closed systems, have a large cost increase since the reactor material cost is relatively high (Fig. 4-3). The liquid sorption system estimated in 5.2 has a moderate increase due to the relatively small amount of material estimated to store the sorbent and the sorbate in the different staged of the process.

In particular, the closed systems based on $MgCl_2$, Na_2S and the composite material shift from the building user class to the enthusiast user class range of storage capacity costs. The open systems based on the same materials remain below the maximum storage capacity costs acceptable from the building user.

To conclude, it has to be remarked that, for the sake of comparison, only active material and reactor material costs are estimated and considered in Fig. 5-2. For liquid sorption systems taken from the literature, only active material costs are considered and the energy density is given for one cubic meter of solution after the desorption phase. Other system materials, components and operational costs are not considered in this analysis and they would increase additionally the storage capacity costs of the thermal storages investigated. Existing thermal storage systems evaluated with the abovementioned approach can be found in [55].

6. Conclusions

In this work, ideal sorption heat storage systems are estimated and compared in terms of energy densities and storage capacity costs. A common reference scenario for the analysis has been assumed consisting of a seasonal heat storage for space heating of a passive house located in Amsterdam, the Netherlands.

Five conceptual solid open systems and five closed systems based on different salt hydrates, zeolite 13X, and an ideal composite material have been estimated. Moreover, a conceptual liquid sorption system based on NaOH is compared with the solid sorption systems in the same reference scenario. The results showed that the closed systems are in general more expensive and less compact than the open systems for the assumed reactor layouts, and the liquid system would result in a larger and more expensive system compared to the solid systems based on the ideal composite material and certain salt hydrates. On the contrary, the liquid system would be more affordable compared to systems based on zeolite 13X and the most expensive salt hydrates. Finally, the open system based on the composite material, could represent a valid compromise between energy density and storage capacity costs, assuming a sufficient hydrothermal stability.

From the economic perspective, the active materials cost assumed for the investigated systems are too high for industry users. For implementation in domestic buildings, systems based only on certain pure salt hydrates, on the ideal composite material, and on the liquid sorption system become affordable. When reactor material costs are also considered, the overall system cost, especially for closed solid sorption systems, increases remarkably.

This analysis highlights that the costs for the investigated sorption seasonal heat storage systems, even when considering only the active material and the reactor material costs, are still relatively high for the user classes considered in this work. Especially considering that the cost of auxiliary system components (e.g. the heat exchangers in solid sorption closed systems and the absorber in the liquid sorption system) and the operational costs are not taken into account in this work. The acceptable storage capacity costs used in this analysis are largely affected by the energy prices, which are dependent on multiple factors determining the market conditions. For example, an increase in reference energy costs (REC) would increase the acceptable storage capacity costs. Conversely, if the storage could perform multiple charge/discharge cycles per year, the acceptable storage capacity costs would decrease remarkably. Thus, in the upcoming future, sorption seasonal heat storage systems like the ones investigated in this analysis can become more competitive in the energy sector according to the future energy market conditions.

Acknowledgements

This project receives the support of the European Union, the European Regional Development Fund ERDF, Flanders Innovation & Entrepreneurship and the Province of Limburg. TU/e has received funding from European Union's Horizon 2020 research and innovation programme under grant agreement Nº 657466 (INPATH-TES). The results of this study can contribute to the development of educational material within INPATH-TES.

Appendix A. Equilibrium curves and active materials data

See Table A-1 and Fig. A-1.

Table A-1
Properties of Na_2S ($Na_2S \leftrightarrow Na_2S{\cdot}2H_2O$, $Na_2S{\cdot}2H_2O \leftrightarrow Na_2S{\cdot}5H_2O$, $Na_2S{\cdot}5H_2O \leftrightarrow Na_2S{\cdot}9H_2O$), $SrBr_2$ ($SrBr_2{\cdot}H_2O \leftrightarrow SrBr_2{\cdot}6H_2O$). and zeolite 13X. Reaction enthalpy data from [26].

Na_2S			**$SrBr_2$**		**Zeolite 13X**	
$\rho_{Na2S{\cdot}9H2O}$ [kg/m^3]	1430		$\rho_{SrBr2{\cdot}6H2O}$ [kg/m^3]	2386	$\rho_{Zeolite\ 13X}$ [kg/m^3]	1040
$\rho_{Na2S{\cdot}5H2O}$ [kg/m^3]	1580		$M_{SrBr2{\cdot}6H2O}$ [g/mol]	355.53	$\Delta H_{reaction}$ [kJ/mol(H_2O)]	63
$M_{Na2S{\cdot}9H2O}$ [g/mol]	240.18		Moles of water in solid phase	1↔6	mol(H_2O)/kg(Zeolite 13X)	11
$M_{Na2S{\cdot}5H2O}$ [g/mol]	168.12		mol(H_2O)	5	E_{total} [GJ/m^3(Zeolite 13X)]	0.72
Moles of water in solid phase	0.5↔2	2↔5	$\Delta H_{reaction}$ [kJ/mol(H_2O)]	58.16	$E_{bed,total}$ [GJ/m^3(Zeolite 13X)]	0.36
mol(H_2O)	1.5	3	mol(H_2O)/kg($SrBr_2{\cdot}6H_2O$)	14.06	$C_{material}$ [€/t] [27]	2500
$\Delta H_{reaction}$ [kJ/mol(H_2O)]	72	62.85	T_{eq} [°C]	50.45		
mol(H_2O)/kg($Na_2S{\cdot}5H_2O$)	8.92	17.84	E_{total} [GJ/m^3($SrBr_2{\cdot}6H_2O$)]	1.95		
T_{eq} [°C]	73.84	67.19	$E_{bed,total}$ [GJ/m^3($SrBr_2{\cdot}6H_2O$)]	0.98		
E [GJ/m^3($Na_2S{\cdot}5H_2O$)]	1.01	1.77	$C_{material}$ [€/t] [27]	2400		
E_{total} [GJ/m^3($Na_2S{\cdot}5H_2O$)]	2.79					
$E_{bed,total}$ [GJ/m^3($Na_2S{\cdot}5H_2O$)]	1.39					
$C_{material}$ [€/t] [27]	348					

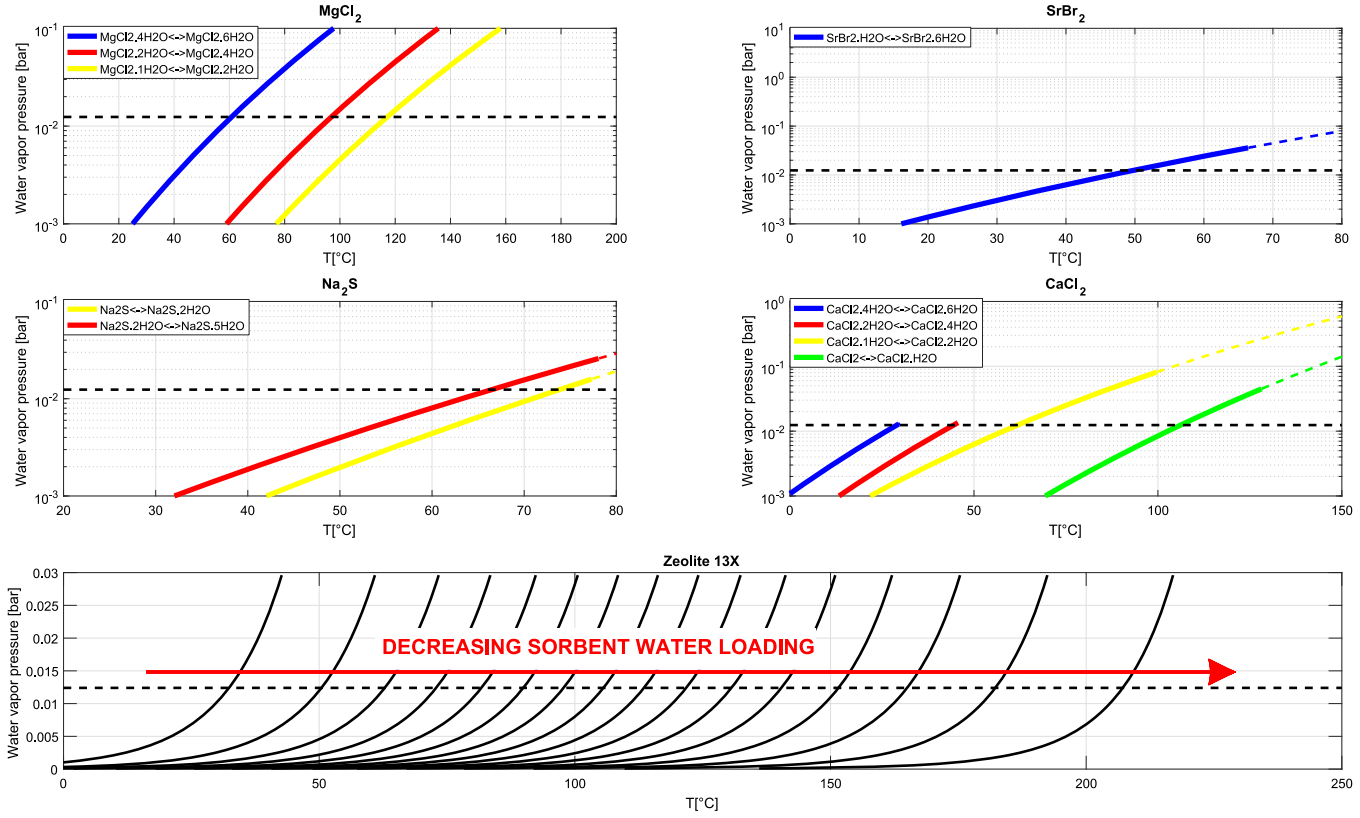

Fig. A-1. Equilibrium curveas for $MgCl_2$ (top left), $SrBr_2$ (top right), Na_2S (bottom left), $CaCl_2$ (bottom right) and adsorption isoteres (black lines) for zeolite 13X (bottom). Dashed line: p(H_2O)=12.4 mbar.

Appendix B. Additional parameters for the systems design

See Table B-1.

Table B-1
Additional assumptions for the systems design estimation.

D_p [mm]	1
ε	0.5
$\eta_{heat\ recovery}$ open system [%]	90
$\rho_{Stainless\ Steel}$ [kg/m^3] [57]	7740
$C_{Stainless\ Steel}$ [€/t] [58]	2500
ρ_{air} [kg/m^3]	1.2
μ_{air} [mPa s]	$1.85 \cdot 10^{-5}$
$c_{p,\ air}$ [J/(kg K)]	1004
M_{H_2O} [g/mol]	18
$c_{p,\ H2O}$ [J/(kg K)]	4186

Appendix C. Estimation of the ideal liquid sorption system

In this analysis, four states of the solution are defined. State 1 represents the storage conditions before the beginning of the sorption process. State 2 represent the beginning of the sorption process, when the solution starts to release heat at the highest sorbent concentration. State 3 represents the solution at the end of the useful heat release. State 3′ represents the solution at the outlet of the absorber, after the further dilution to avoid solidification at $T_{storage}$. Finally, state E represents the evaporator state.

By looking at the phase diagram of NaOH-H_2O [59] (Fig. C-1), it is possible to see that at $T_{storage}$, the solution can be stored at a maximum concentration of approximately 48 wt%$_{NaOH}$ (1). This has to be the maximum concentration in the storage system in order to avoid crystallization. At higher concentrations of NaOH at $T_{storage}$, the solidification curve would be crossed. According to Fig. C-2 and the assumptions in this analysis, the minimum concentration of NaOH in order to produce heat above 35 °C is 40 wt%$_{NaOH}$ (3). However, to avoid crystallization at $T_{storage}$, the solution has to be diluted further in order to reach a concentration lower than 32 wt%$_{NaOH}$ (3′).

The useful concentration difference in the absorber is 8 wt%$_{NaOH}$, while the total concentration difference is 16 wt%$_{NaOH}$. During discharge, the

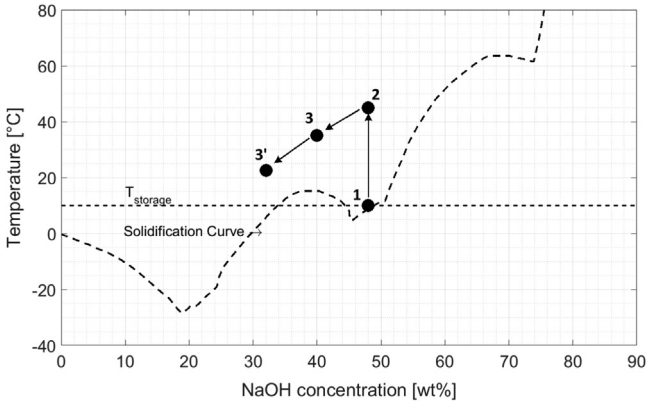

Fig. C-1. Boiling and solidifying temperatures of aqueous caustic soda solutions. The system states during the evaporation process are 1: strong solution in the storage tank, 2: solution at the beginning of the absorption process, 3: solution at the end of the absorption process that produces useful heat above 35 °C, 3′: solution diluted up to the minimum concentration in the system to prevent crystallization during storage.
Partially adapted from [59].

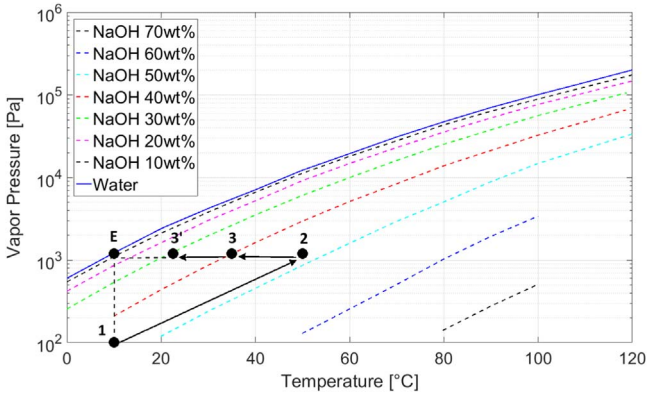

Fig. C-2. Vapor pressure vs temperature curves for NaOH-H_2O absorption couple. The system states during the evaporation process are 1: strong solution in the storage tank, 2: solution at the beginning of the absorption process, 3: solution at the end of the absorption process that produces useful heat above 35 °C, 3′: solution diluted up to the minimum concentration in the system to prevent crystallization during storage, E: the evaporator state.
Partially adapted from [60].

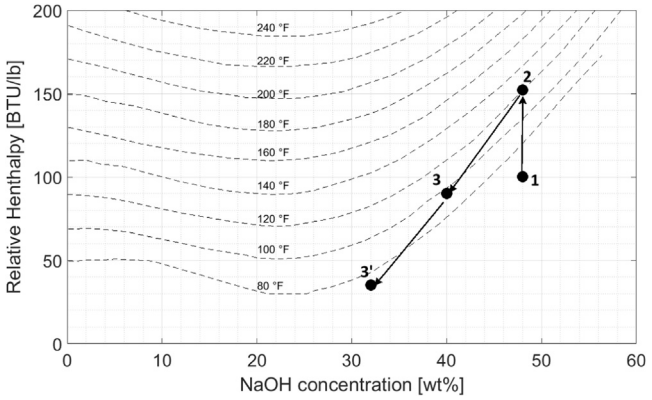

Fig. C-3. Relative enthalpy of NaOH solutions. The system states during the evaporation process are 1: strong solution in the storage tank, 2: solution at the beginning of the absorption process, 3: solution at the end of the absorption process that produces useful heat above 35 °C, 3′: solution diluted up to the minimum concentration in the system to prevent crystallization during storage.
Partially adapted from [59].

Table C-1
Enthalpies of the solution at state 1 and 3; and saturated water vapor enthalpy at system conditions.

h_1 [kJ/kg$_{sol}$]	232.6
h_3 [kJ/kg$_{sol}$]	204.69
h_{vap} [kJ/kg]	2519.22

Table C–2
Tanks parameters of the ideal liquid sorption system. An aspect ratio between the tanks diameter and height equal to 1 has been assumed.

	High Concentration Tank (HCT)	**Low Concentration Tank (LCT)**	**Sorbate Tank (ST)**
V_{tank} [m^3]	15.2	25.3	10.2
D_{tank} [m]	2.68	3.18	2.35
C_{tank} [€]	28.4	34.6	24.5

concentrated solution at 48 wt%$_{NaOH}$ goes into the absorber from the storage tank (1→2). The solution concentration decreases up to the minimum concentration (40 wt%) in order to produce heat above 35 °C (2→3). Then, the solution is further diluted up to 32 wt% (3→3′) to avoid crystallization at storage conditions (see Fig. C-1). The required desorption temperature for this system, assuming a condenser temperature of 30 °C (p_{H2O}=4.2 kPa) as Liu et al. [50], would be approximately 75 °C.

The useful energy produced in the absorber is considered to be only the one extracted from 2→3. The energy released during the further dilution 3→3′ is not considered. The energy balance can be done by considering the state of the solution during the storage immediately before the discharge phase at state 1, and state 3.

$$e_{1\to3,T>35°C} = m_1 \cdot h_1 + (m_3 - m_1)\cdot h_{vap} - m_3 \cdot h_3 = \left(\frac{1}{0.48}\right)\cdot 232.6 + \left(\frac{1}{0.4} - \frac{1}{0.48}\right)\cdot 2519.228 - \frac{1}{0.4}\cdot 204.69 = 1022.535 \quad kJ/kg_{NaOH} \tag{C.1}$$

With $m = \frac{1}{x_{NaOH}}$ the relative masses in [kg$_{solution}$/kg$_{absorbent}$], x the mass concentration of absorbent into the solution, h the solution sensible enthalpy and h_{vap} the water vapor enthalpy at the evaporator state (p=p_{sat} , T=10 °C). The useful energy balance of the absorber can be solved considering the enthalpies calculated from Fig. C-3, and presented in Table C-1, together with the water vapor enthalpy at system conditions. On hydration of NaOH, energy produced per cubic meter of absorbent above 35 °C is:

$$E_{NaOH} = e_{1\to3}\cdot\rho_{NaOH} = 1022535\cdot 2130\cdot\frac{1}{10^9} = 2.18 \quad GJ/m^3_{NaOH} \tag{C.2}$$

In order to satisfy the space heating energy demand of one year in the reference scenario, the amount of NaOH required is:

$$V_{NaOH} = E_{NaOH}\cdot ESH = \frac{10}{2.18} = 4.587 \quad m^3_{NaOH} \tag{C.3}$$

Then, in order to calculate the energy density of the solution, the amount of water present at the most diluted concentration in the system is estimated as:

$$V_{H_2O,weak} = \frac{x_{H_2O}}{x_{NaOH}}\cdot\frac{\rho_{NaOH}}{\rho_{H_2O}} = \frac{(1 - x_{NaOH})}{x_{NaOH}}\cdot\frac{\rho_{NaOH}}{\rho_{H_2O}} = \frac{(1-0.32)}{0.32}\cdot\frac{2130}{1000} = 4.526 \quad \frac{m^3_{H_2O}}{m^3_{NaOH}} \tag{C.4}$$

At the abovementioned conditions, the solution energy density is:

$$E_{sol,weak} = \frac{E_{NaOH}}{V_{NaOH} + V_{H_2O}} = \frac{2.18}{1 + 4.526} = 0.39 \quad GJ/m^3_{sol} \tag{C.5}$$

Making use of equation (C.4), the amount of water in the strong solution (x_{NaOH}=48$wt\%$) can be found equal to $V_{H2O,strong}$=2.307 m^3_{H2O}/m^3_{NaOH}. The amount of sorbate that has to be stored separated from the solution is equal to $V_{H2O,pure}$=2.219 m^3_{H2O}/m^3_{NaOH}.

The total amount of water in the strong solution tank can be found according to equation (C.6).

$$V_{H2O,HCT} = V_{NaOH} \cdot V_{H2O,strong} = 10.58 \quad m^3_{H_2O} \tag{C.6}$$

The volumes of the low concentration tank and of the pure sorbate tank can be found similarly and are displayed in Table C-2.

The energy density of the weak solution does not give a fair estimation of the system energy density. In particular, the system has to make use of at least three storage tanks. One tank has to store the strong solution (high concentration tank HCT), a second tank has to store the pure sorbate (sorbate tank ST), and a third tank has to store the weak solution (low concentration tank LCT). By adding the three volumes that the tanks have to store, a more realistic value ($E_{sol,system}$) of the system energy density can be found according to equation (C.7).

$$E_{sol,\ system} = \frac{ESH}{2 \cdot V_{NaOH} + V_{H2O,HCT} + V_{H2O,ST} + V_{H2O,LCT}} = \frac{ESH}{V_{HCT} + V_{LCT} + V_{ST}} = \frac{10}{15.2 + 25.3 + 10.2} = 0.20 \quad GJ/m^3_{sol} \tag{C.7}$$

The active material cost in the reference scenario (2.1) is calculated considering only the NaOH cost (Table 5-1) :

$$C_{NaOH} = \frac{ESH}{E_{NaOH}} \cdot \rho_{NaOH} \cdot price_{NaOH} = \frac{10 \cdot 10^9 [GJ]}{2.18 \cdot 10^9 \left[\frac{GJ}{m^3_{NaOH}}\right]} \cdot 2130 \left[\frac{kg_{NaOH}}{m^3_{NaOH}}\right] \cdot 0.4[\text{kg}] = 3.91 \quad k€ \tag{C.8}$$

The storage capacity cost by taking only into account the active material is found by dividing the absorbent cost with the energy delivered for the space heating system ESH, assuming that only one cycle is performed every year.

$$C_{SSC,NaOH} = \frac{C_{NaOH}}{ESH} = 1.41 \quad €/\text{kWh}_{cap} \tag{C.9}$$

The reactor material costs are estimated assuming that the system consists mainly of three stainless steel 316 storage tanks with a thickness of 3 mm, an aspect ratio diameter/height of approximately 1, and the cylinder ends consisting of domes with a 0.05 m height. The tanks cost are estimated by assuming the same cost and density of stainless steel 316 as in Section 3 (ρ_{SS} =7740 kg/m^3, C_{SS} =2.5 €/kg). The storage capacity cost including the material cost for the storage can be calculated according to equation (C.10):

$$C_{SSC,NaOH+tanks} = \frac{C_{NaOH} + C_{tank,HCT} + C_{tank,LCT} + C_{tank,ST}}{ESH} = 1.44 \quad €/\text{kWh}_{cap} \tag{C.10}$$

The absorber, which is assumed to be small compared to the storage tanks, is not taken into account in this cost estimation.

References

[1] Kalaiselvam S, Parameshwaran R. Energy Storage. Therm. energy storage Technol. Sustain - Syst Des Assess Appl. Elsevier Inc; 2014. p. 21–56. http://dx.doi.org/10.1016/B978-0-12-417291-3.00002-5.

[2] Lund H, Werner S, Wiltshire R, Svendsen S, Thorsen JE, Hvelplund F, et al. 4th Generation District Heating (4GDH). Integrating smart thermal grids into future sustainable energy systems. Energy 2014;68:1–11. http://dx.doi.org/10.1016/j.energy.2014.02.089.

[3] Gao L, Zhao J, Tang Z. A review on borehole seasonal solar thermal energy storage. Energy Procedia, 70. Elsevier B.V; 2015. p. 209–18. http://dx.doi.org/10.1016/j.egypro.2015.02.117.

[4] Pielichowska K, Pielichowski K. Phase change materials for thermal energy storage. Prog Mater Sci 2014;65:67–123. http://dx.doi.org/10.1016/j.pmatsci.2014.03.005.

[5] Sharif MKA, Al-abidi AA, Mat S, Sopian K, Ruslan MH. Review of the application of phase change material for heating and domestic hot water systems. Renew Sustain Energy Rev 2015;42:557–68. http://dx.doi.org/10.1016/j.rser.2014.09.034.

[6] Scapino L, Zondag HA, Van Bael J, Diriken J, Rindt CCM. Sorption heat storage for long-term low-temperature applications: a review on the advancements at material and prototype scale. Appl Energy 2017;190:920–48. http://dx.doi.org/10.1016/j.apenergy.2016.12.148.

[7] Lapillonne B, Sebi C, Pollier K, Mairet N. Energy efficiency trends in buildings in the EU; 2015.

[8] Yu N, Wang RZ, Wang LW. Sorption thermal storage for solar energy. Prog Energy Combust Sci 2013;39:489–514. http://dx.doi.org/10.1016/j.pecs.2013.05.004, [Review].

[9] Aydin D, Casey SP, Riffat S. The latest advancements on thermochemical heat storage systems. Renew Sustain Energy Rev 2015;41:356–67. http://dx.doi.org/10.1016/j.rser.2014.08.054.

[10] Ding Y, Riffat S. Thermochemical energy storage technologies for building applications: a state-of-the-art review. Int J Low-Carbon Technol 2012;8:106–16. http://dx.doi.org/10.1093/ijlct/cts004.

[11] N'Tsoukpoe KE, Liu H, Le Pierrès N, Luo L. A review on long-term sorption solar energy storage. Renew Sustain Energy Rev 2009;13:2385–96. http://dx.doi.org/10.1016/j.rser.2009.05.008.

[12] Solé A, Martorell I, Cabeza LF. State of the art on gas–solid thermochemical energy storage systems and reactors for building applications. Renew Sustain Energy Rev 2015;47:386–98. http://dx.doi.org/10.1016/j.rser.2015.03.077.

[13] N'Tsoukpoe KE, Restuccia G, Schmidt T, Py X. The size of sorbents in low pressure sorption or thermochemical energy storage processes. Energy 2014;77:983–98. http://dx.doi.org/10.1016/j.energy.2014.10.013.

[14] Solé A, Miró L, Barreneche C, Martorell I, Cabeza LF. Corrosion Test of Salt Hydrates and Vessel Metals for Thermochemical Energy Storage. Energy Procedia 2014;48:431–5. http://dx.doi.org/10.1016/j.egypro.2014.02.050.

[15] Zondag HA. Sorption Heat Storage. In: Soerensen B, editor. Sol. Energy Storage1st ed. Elsevier; 2015. p. 135–54. http://dx.doi.org/10.1016/B978-0-12-409540-3.00006-2.

[16] Abedin AH, Rosen MA. Closed and open thermochemical energy storage: energy- and exergy-based comparisons. Energy 2012;41:83–92. http://dx.doi.org/10.1016/j.energy.2011.06.034.

[17] Hauer A. Sorption Storages for Solar Thermal Energy – Possibilities and Limits, 2008. Lisbon, Portugal: Eurosun; 2008. p. 1–8.

[18] Scapino L, Zondag HA, Van Bael J, Diriken J, Rindt CCM. Sorption heat storage for long-term low-temperature applications: a review on the advancements at material and prototype scale. Appl Energy 2017;190:920–48. http://dx.doi.org/10.1016/j.apenergy.2016.12.148.

[19] Pinel P, Cruickshank C a, Beausoleil-Morrison I, Wills A. A review of available methods for seasonal storage of solar thermal energy in residential applications. Renew Sustain Energy Rev 2011;15:3341–59. http://dx.doi.org/10.1016/j.rser.2011.04.013.

[20] Xu J, Wang RZ, Li Y. A review of available technologies for seasonal thermal energy storage. Sol Energy 2013;103:610–38. http://dx.doi.org/10.1016/j.solener.2013.06.006.

[21] Ovchinnikov P, Borodiņecs A, Strelets K. Utilization potential of low temperature hydronic space heating systems: a comparative review. Build Environ 2016;112:88–98. http://dx.doi.org/10.1016/j.buildenv.2016.11.029.

[22] Ferchaud CJ, Zondag HA, de Boer R, Rindt CCM. Characterization of the sorption process in thermochemical materials for seasonal solar heat storage application. In: nostock 2012 Proceedings of the 12th International Conference Energy Storage, p. 1–10; 2012.

[23] Ferchaud CJ, Scherpenborg RAA, Zondag HA, de Boer R. Thermochemical Seasonal Solar Heat Storage in Salt Hydrates for Residential Applications – Influence of the Water Vapor Pressure on the Desorption Kinetics of $MgSO_4.7H_2O$. Energy Procedia, 57. Elsevier B.V; 2014. p. 2436–40. http://dx.doi.org/10.1016/j.egypro.2014.10.252.

[24] Zondag HA, Kikkert B, Smeding S, de Boer R, Bakker M. Prototype thermochemical heat storage with open reactor system. Appl Energy 2013;109:360–5. http://dx.doi.org/10.1016/j.apenergy.2013.01.082.

[25] de Jong A-J, Trausel F, Finck C, Van Vliet L, Cuypers R. Thermochemical heat storage - System design issues. Energy Procedia, 48. Elsevier B.V; 2014. p. 309–19.

http://dx.doi.org/10.1016/j.egypro.2014.02.036.
[26] Wagemann DD, Evans WH, Parker VB, Schumm RH, Halow I, Baily SM, et al. [Supplem]NBS Tables Chem Thermodyn Prop: Sel Values Inorg C1 C2 Org Subst SI units 1982;11, [Supplem].
[27] Trausel F, de Jong A-J, Cuypers R. A review on the properties of salt hydrates for thermochemical storage. SHC 2013, International Conference Sol. Heat. Cool. Build. Ind., vol. 48, Elsevier B.V, p. 447–52. doi:http://dx.doi.org/10.1016/j.egypro.2014.02.053; 2014.
[28] Gaeini M, Zondag H a. Non-Isothermal Kinet Zeolite Water Vap Adsorpt Into a Packed Bed Lab Scale Thermochem 2014:1–11.
[29] Expanded Vermiculite Price and Density n.d. ⟨http://www.alibaba.com⟩ [accessed 8 April 2016].
[30] N'Tsoukpoe KE, Rammelberg HU, Lele AF, Korhammer K, Watts BA, Schmidt T, et al. A review on the use of calcium chloride in applied thermal engineering. Appl Therm Eng 2015;75:513–31. http://dx.doi.org/10.1016/j.applthermaleng.2014.09.047.
[31] van Essen VM, Cot-Gores J, Bleijendaal LPJ, Zondag HA, Schuitema R, Bakker M. et al. Characterization of Salt Hydrates for Compact Seasonal Thermochemical Storage. ASME 2009 In: Proceedings of the 3rd International Conference Energy Sustain, p. 825–30. doi:http://dx.doi.org/10.1115/ES2009-90289; 2009.
[32] Ponomarenko IV, Glaznev IS, Gubar AV, Aristov YI, Kirik SD. Synthesis and water sorption properties of a new composite "CaCl2 confined into SBA-15 pores.". Microporous Mesoporous Mater 2010;129:243–50. http://dx.doi.org/10.1016/j.micromeso.2009.09.023.
[33] Korhammer K, Druske M-M, Fopah-Lele A, Rammelberg HU, Wegscheider N, Opel O, et al. Sorption and thermal characterization of composite materials based on chlorides for thermal energy storage. Appl Energy 2016;162:1462–72. http://dx.doi.org/10.1016/j.apenergy.2015.08.037.
[34] Tokarev M, Gordeeva L, Romannikov V, Glaznev I, Aristov Y. New composite sorbent CaCl2 in mesopores for sorption cooling/heating. Int J Therm Sci 2002;41:470–747. http://dx.doi.org/10.1016/S1290-0729(02)01339-X.
[35] Ristić A, Maučec D, Henninger SK, Kaučič V. New two-component water sorbent CaCl2-FeKIL2 for solar thermal energy storage. Microporous Mesoporous Mater 2012;164:266–72. http://dx.doi.org/10.1016/j.micromeso.2012.06.054.
[36] Barreneche C, Fernández AI, Cabeza LF, Cuypers R. Thermophysical characterization and thermal cycling stability of two TCM: cacl2 and zeolite. Appl Energy 2014;137:726–30. http://dx.doi.org/10.1016/j.apenergy.2014.09.025.
[37] Chan K, Chao CYH, Bahrami M. Heat and Mass Transfer Characteristics of a Zeolite 13X/CaCl2 Composite Adsorbent in Adsorption Cooling Systems. ASME 2012 In: Proceedings of the 6th International Conference Energy Sustain 10th Fuel Cell Sci Eng Technol Conference:1–10; 2012.
[38] Rammelberg HU, Schmidt T, Ruck WKL. Hydration and dehydration of salt hydrates and hydroxides for thermal energy storage - Kinetics and energy release. Energy Procedia, 30. Elsevier B.V; 2012. p. 362–9. http://dx.doi.org/10.1016/j.egypro.2012.11.043.
[39] Jänchen J, Ackermann D, Weiler E, Stach H, Brösicke W. Calorimetric investigation on zeolites, AlPO4′s and CaCl 2 impregnated attapulgite for thermochemical storage of heat. Thermochim Acta 2005;434:37–41. http://dx.doi.org/10.1016/j.tca.2005.01.009.
[40] Casey SP, Elvins J, Riffat S, Robinson A. Salt impregnated desiccant matrices for "open" thermochemical energy storage—Selection, synthesis and characterisation of candidate materials. Energy Build 2014;84:412–25. http://dx.doi.org/10.1016/j.enbuild.2014.08.028.
[41] Gordeeva L, Grekova A, Krieger T, Aristov Y. Composites "binary salts in porous matrix" for adsorption heat transformation. Appl Therm Eng 2013;50:1633–8. http://dx.doi.org/10.1016/j.applthermaleng.2011.07.040.
[42] Donkers PAJ. Experimental study on thermochemical heat storage materials. Eindh Univ Technol 2015.
[43] Stainless steel 316 sheet n.d. ⟨www.alibaba.com⟩.
[44] Merzkirch A, Maas S, Scholzen F, Waldmann D. Field tests of centralized and decentralized ventilation units in residential buildings - Specific fan power, heat recovery efficiency, shortcuts and volume flow unbalances. Energy Build 2016;116:373–83. http://dx.doi.org/10.1016/j.enbuild.2015.12.008.
[45] Donkers PAJ, Pel L, Adan OCG. Experimental studies for the cyclability of salt hydrates for thermochemical heat storage. J Energy Storage 2016;5:25–32. http://dx.doi.org/10.1016/j.est.2015.11.005.
[46] Zondag HA, van Essen VM, Bleijendaal LPJ, Kikkert B, Bakker M. Application of $MgCl_2{\cdot}6H_2O$ for thermochemical seasonal solar heat storage. 5th International Renew. Energy Storage Conference IRES 2010, Berlin, Germany; 2010.
[47] Eurostat. Electricity and gas prices, second half of year, 2013–15 (EUR per kWh) 2016. ⟨http://ec.europa.eu/eurostat/statistics-explained/index.php/File:Electricity_and_gas_prices,_second_half_of_year,_2013%25E2%2580%259315_(EUR_per_kWh)_YB16.png⟩ [accessed 25 November 2016].
[48] Fujioka K, Suzuki H. Thermophysical properties and reaction rate of composite reactant of calcium chloride and expanded graphite. Appl Therm Eng 2013;50:1627–32. http://dx.doi.org/10.1016/j.applthermaleng.2011.08.024.
[49] Liu H, Le Pierrès N, Luo L Seasonal storage of solar energy for house heating by different absorption couples. In: Proceedings of the 11th International Conference Energy Storage, Effstock, Stockholm, Sweden: n.d., p. 1–8.
[50] Liu H, N'Tsoukpoe KE, Nolwenn LP, Luo L. Evaluation of a seasonal storage system of solar energy for house heating using different absorption couples. Energy Convers Manag 2011;52:2427–36. http://dx.doi.org/10.1016/j.enconman.2010.12.049.
[51] Srikhirin P, Aphornratana S, Chungpaibulpatana S. A review of absorption refrigeration technologies. Renew Sustain Energy Rev 2001;5:343–72. http://dx.doi.org/10.1016/S1364-0321(01)00003-X.
[52] Siddiqui MU, Said S aM. A review of solar powered absorption systems. Renew Sustain Energy Rev 2015;42:93–115. http://dx.doi.org/10.1016/j.rser.2014.10.014.
[53] Wu W, Wang B, Shi W, Li X. An overview of ammonia-based absorption chillers and heat pumps. Renew Sustain Energy Rev 2014;31:681–707. http://dx.doi.org/10.1016/j.rser.2013.12.021.
[54] Liquid sorption materials prices n.d. ⟨www.alibaba.com⟩ [accessed 15 February 2016].
[55] Rathgeber C, Hiebler S, Lävemann E, Dolado P, Lazaro A, Gasia J. et al. IEA SHC Task 42/ ECES Annex 29 – A simple tool for the economic evaluation of thermal energy storages. SHC 2015 , International Conference Sol. Heat. Cool. Build. Ind; 2015.
[56] Rathgeber C, Lävemann E, Hauer A. Economic top–down evaluation of the costs of energy storages—A simple economic truth in two equations. J Energy Storage 2015;2:43–6. http://dx.doi.org/10.1016/j.est.2015.06.001.
[57] Stainless steel density n.d. ⟨www.engineeringtoolbox.com/metal-alloys-densities-d_50.html⟩ Accessed 18 February 2016.
[58] Stainless steel prices n.d. ⟨www.alibaba.com⟩ Accessed 18 February 2016.
[59] Oxychem Caustic. Soda handbook. Dallas, Texas (US): Oxychem; 2013.
[60] Weber R, Dorer V. Long-term heat storage with NaOH. Vacuum 2008;82:708–16. http://dx.doi.org/10.1016/j.vacuum.2007.10.01.